

Exploring the enzymatic degradation of poly(glycerol adipate)

Swainson, Sadie M.E.; Taresco, Vincenzo; Pearce, Amanda K.; Clapp, Lucie H.; Ager, B.; McAllister, Mark; Bosquillon, Cynthia; Garnett, Martin C.

DOI:

[10.1016/j.ejpb.2019.07.015](https://doi.org/10.1016/j.ejpb.2019.07.015)

License:

Creative Commons: Attribution-NonCommercial-NoDerivs (CC BY-NC-ND)

Document Version

Peer reviewed version

Citation for published version (Harvard):

Swainson, SME, Taresco, V, Pearce, AK, Clapp, LH, Ager, B, McAllister, M, Bosquillon, C & Garnett, MC 2019, 'Exploring the enzymatic degradation of poly(glycerol adipate)', *European Journal of Pharmaceutics and Biopharmaceutics*, vol. 142, pp. 377-386. <https://doi.org/10.1016/j.ejpb.2019.07.015>

[Link to publication on Research at Birmingham portal](#)

Publisher Rights Statement:

Sainson, S. et al (2019) Exploring the enzymatic degradation of poly(glycerol adipate), *European Journal of Pharmaceutics and Biopharmaceutics*, 142: 377-386; <https://doi.org/10.1016/j.ejpb.2019.07.015>

General rights

Unless a licence is specified above, all rights (including copyright and moral rights) in this document are retained by the authors and/or the copyright holders. The express permission of the copyright holder must be obtained for any use of this material other than for purposes permitted by law.

- Users may freely distribute the URL that is used to identify this publication.
- Users may download and/or print one copy of the publication from the University of Birmingham research portal for the purpose of private study or non-commercial research.
- User may use extracts from the document in line with the concept of 'fair dealing' under the Copyright, Designs and Patents Act 1988 (?)
- Users may not further distribute the material nor use it for the purposes of commercial gain.

Where a licence is displayed above, please note the terms and conditions of the licence govern your use of this document.

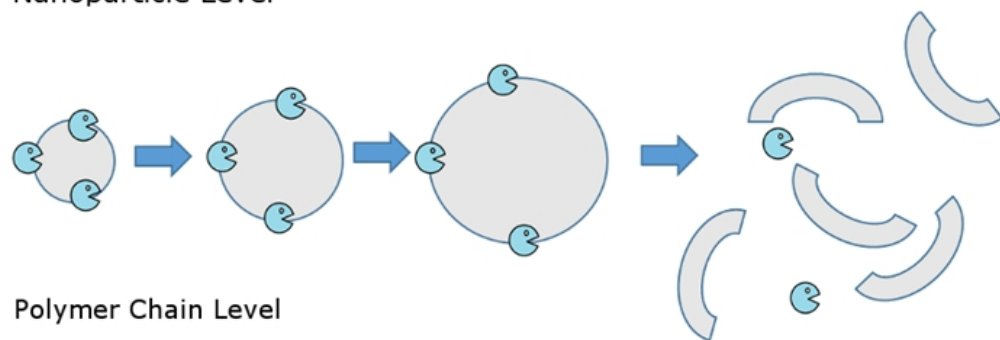
When citing, please reference the published version.

Take down policy

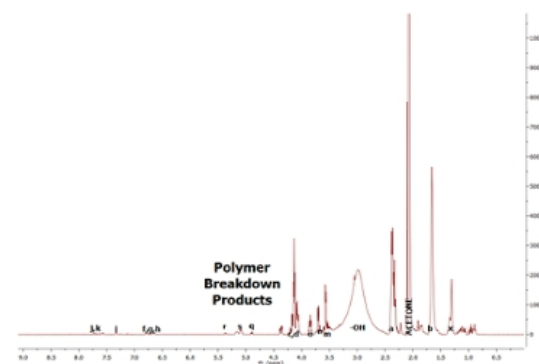
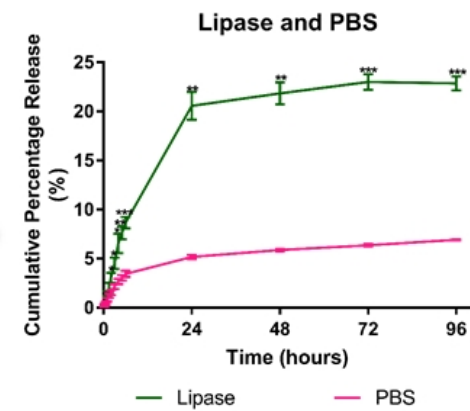
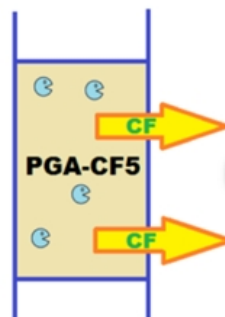
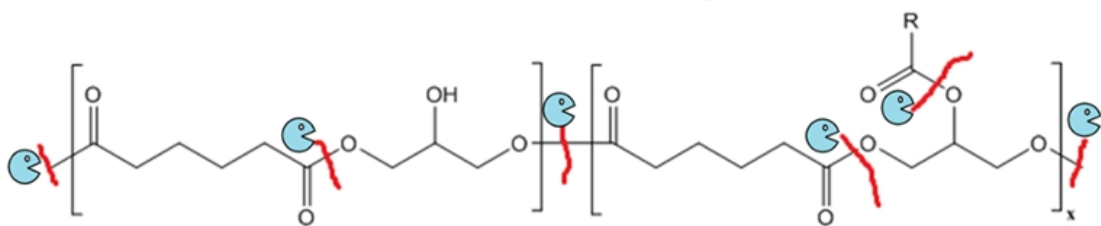
While the University of Birmingham exercises care and attention in making items available there are rare occasions when an item has been uploaded in error or has been deemed to be commercially or otherwise sensitive.

If you believe that this is the case for this document, please contact UBIRA@lists.bham.ac.uk providing details and we will remove access to the work immediately and investigate.

Nanoparticle Level



Polymer Chain Level



Exploring the Enzymatic Degradation of Poly(Glycerol Adipate)

Sadie M E Swainson¹, Vincenzo Taresco¹, Amanda K Pearce¹, Lucie H Clapp², Barry Ager³, Mark McAllister³, Cynthia Bosquillon¹, and Martin C Garnett^{1*}

1. School of Pharmacy, University of Nottingham, Nottingham, NG7 2RD
2. Department of Medicine, University College London, London, WC1E 6JF
3. Drug Product Design, Pfizer Ltd, Sandwich, CT13 9ND

Abstract

Poly(glycerol adipate) (PGA) is a biodegradable, biocompatible, polymer with a great deal of potential in the field of drug delivery. Active drug molecules can be conjugated to the polymer backbone or encapsulated in self-assembled nanoparticles for targeted and systemic delivery. Here, a range of techniques have been used to characterise the enzymatic degradation of PGA extensively for the first time and to provide an indication of the way the polymer will behave and release drug payloads *in vivo*. Dynamic Light Scattering was used to monitor change in nanoparticle size, indicative of degradation. The release of a fluorescent dye, coupled to PGA, upon incubation with enzymes was measured over a 96 hour period as a model of drug release from polymer drug conjugates. The changes to the chemical structure and molecular weight of PGA following enzyme exposure were characterised using FTIR, NMR and GPC. These techniques provided evidence of the biodegradability of PGA, its susceptibility to degradation by a range of enzymes commonly found in the human body and the polymer's potential as a drug delivery platform.

Key Words: Poly(Glycerol Adipate), Enzymatic Degradation, Polyester, Biodegradable, Polymer Modification, Breakdown

1. Introduction

Poly(glycerol adipate) (PGA) is synthesised by enzymatic polymerisation from glycerol and either divinyl adipate, dimethyl adipate or adipic acid, using Novozym 435 lipase as the catalyst, allowing a high degree of control over the final product.[1–4] Enzymatic polymerisation is an emerging area of research which provides several benefits as a method

60
61
62 for producing materials for drug delivery compared with more traditional synthesis methods.
63
64 The avoidance of metal catalysts removes the risk of toxic metals in the final product, while
65 the use of an enzyme catalyst enables high levels of enantio-, chemo- and regioselectivity
66 using mild reaction conditions.[1] PGA self-assembles to form nanoparticles[5] which, with
67 varying levels of stearic acid modification, have been shown to have low cytotoxicity in HL-
68 60 and HepG₂ cells.[6,7] Unmodified PGA and PGA with a range of amino acid
69 modifications have also been shown to have negligible lytic activity in a haemolytic assay.[8]
70
71 The presence of the pendant –OH group in the polymer backbone allows for the conjugation
72 of molecules with a variety of functional groups through simple coupling reactions,
73 influencing the physicochemical properties of PGA and its ability to encapsulate a variety of
74 drugs.[6,8–10] These changes to the polymer as a result of the modifications suggest the
75 enzymatic degradation will be affected due to the enhanced stability, altered hydrophobicity
76 and increased steric hindrance, leading to a potential for tunable breakdown and release *in*
77 *vivo*. Previously, this has been demonstrated through functionalisation of PGA with N-acyl
78 amino acids via Steglich Esterification.[8] Additionally, the drug molecules
79 indomethacin,[11] methotrexate[12] and ibuprofen[13] have been successfully coupled to the
80 polymer backbone. The low toxicity of PGA coupled with the ease with which it can be
81 synthesised, functionalised with drug molecules and formulated into nanoparticles means it
82 shows great potential as a polymeric platform for both targeted and systemic drug delivery.
83
84
85
86
87
88
89
90
91
92

93
94 It is important to understand the degradation properties of polymers for a number of reasons.
95 From a safety point of view, an awareness of likely breakdown products facilitates the
96 prediction of potential *in vivo* toxicity. Taking PGA as an example, the breakdown products
97 would be expected to be the starting materials, glycerol and adipic acid, as the ester bond
98 represents a fairly weak and susceptible point of cleavage;[1,6,14–17] however without
99 investigation into these breakdown products it is not possible to guarantee the
100 biocompatibility of this polymer. Furthermore, knowledge of the cleavage of the pendant side
101 chains, and the resultant breakdown products, will enable prediction of the likely *in vivo*
102 safety profile, prior to cytotoxicity testing of the breakdown products themselves. Secondly,
103 polymers can be formulated into nano- and microparticles; the breakdown of these particles
104 will affect the mechanisms by which they are cleared from the body[18] and the release of
105 drug payloads. In terms of efficacy, any drug coupled to or encapsulated within a polymer
106 tends to require release in order to achieve therapeutic efficacy.[14,15,19] Consequently,
107
108
109
110
111
112
113
114
115
116
117
118

119
120
121 understanding the way in which this release takes place will inform the design of dosage
122 regimens and subsequent pharmacokinetic experiments. Additionally, susceptibility or indeed
123 a resistance to particular enzymes may impact on the suitability of a specific polymer for
124 different routes of administration and disease targets.[15] Understanding the enzymatic
125 breakdown of PGA and consequently the way it will behave *in vivo* will help to inform any
126 future dosage form design and provide an indication of the safety and efficacy of
127 formulations prior to costly *in vitro* and *in vivo* experiments.
128
129
130
131
132

133 Previously, the release of methotrexate from a PGA-drug conjugate has been studied in the
134 presence of porcine carboxylesterase. The enzyme was seen to increase the release of
135 methotrexate compared with buffer alone over a period of seven days.[12] This work
136 suggested the polymer was susceptible to enzymatic but did not focus on the nature of this
137 degradation in detail or examine the degradation products. Additionally, the degradation of
138 poly(glycerol sebacate) (PGS), a polymer with structural similarity to PGA, has been studied
139 by several groups. However, it is worth noting that PGS is a cross-linked polymer, whereas
140 the PGA in the present study is not cross-linked and largely linear.[20–22] PGS is an
141 elastomer which may be of utility as a tissue scaffold and consequently degradation
142 experiments have tended to focus on bulk characteristics such as the change in film weight
143 and thickness over a period of hours or days. In the case of tissue scaffolds, degradation if too
144 rapid, tends to be seen as a disadvantage. However, as previously mentioned, for drug
145 delivery breakdown of the polymer at the target site is greatly advantageous.
146
147
148
149
150
151
152
153
154

155 The enzymatic degradation, in the presence of six enzymes, of PGA and a selection of amino
156 acid modified polymers has been studied in detail here for the first time alongside two new
157 modifications of PGA; PGA-Carboxyfluorescein, at two levels of substitution, and PGA-
158 poly(ethylene glycol) (PGA-PEG). Pancreatin, pepsin, lipase and trypsin were selected as
159 examples of gastrointestinal enzymes in order to give an indication of the general degradation
160 behaviour of the polymer and to assess the potential future suitability of PGA for
161 encapsulation or coating of oral dosage forms. Esterase was selected as it can be detected in
162 many areas of the body whereas elastase is associated with acute and chronic inflammation in
163 many diseases.[23] A range of techniques has been employed to allow a comprehensive
164 evaluation of the enzymatic degradation behaviour of PGA and relative susceptibility to
165 different enzymes. Dynamic Light Scattering (DLS) was used as a rapid screening method to
166 provide information about particle breakdown and to facilitate the selection of enzyme
167
168
169
170
171
172
173
174
175
176
177

178 concentrations and conditions. A fluorescent dye, carboxyfluorescein, coupled to the
179 polymer, was used as a model of polymer drug conjugates, and as a model for other pendant
180 groups esterified to the free hydroxyl group, in order to study release over time. Finally,
181 Nuclear Magnetic Resonance (NMR), Fourier-Transform Infra-Red (FTIR) and Gel
182 Permeation Chromatography (GPC) were combined to characterise the breakdown of the
183 polymer and identify the breakdown products.
184
185
186
187
188
189

190 191 192 **2. Materials & Methods**

193 194 **2.1 Materials**

195 Tetrahydrofuran (THF, HPLC grade), petroleum ether (reagent grade), acetone (HPLC
196 grade), dimethylformamide (DMF, HPLC grade), sodium hydroxide (NaOH, 2 M), HEPES
197 and boric acid were purchased from Fisher Scientific (Loughborough, UK). Sodium Benzoate
198 (0.1%) was purchased from Alfa Aesar (Heysham, UK). Divinyl adipate was purchased from
199 Tokyo Chemical Industry (Oxford, UK). Acetone-d₆ was purchased from Acros Organics
200 (Geel, Belgium). Novozym 435 (immobilised on acrylic resin), glycerol, 5(6)-
201 carboxyfluorescein (CF), poly(ethylene glycol) (PEG) methyl ether, 4-
202 dimethylaminopyridine (DMAP), N,N'-dicyclohexylcarbodiimide (DCC), phosphate
203 buffered saline (PBS) tablets, Trizma base, potassium phosphate monobasic, hydrochloric
204 acid (HCl, 5 M), sodium chloride, N-succinyl-L-Ala-Ala-Ala-p-nitroanilide, ethyl butyrate,
205 4-methylumbelliferyl butyrate, 4-methyl umbelliferone, N α -benzoyl-L-arginine ethyl ester,
206 deuterium oxide and sodium phosphate monobasic were purchased from Sigma-Aldrich
207 (Poole, UK). Elastase from porcine pancreas Type I (≥ 4.0 units/mg protein), esterase from
208 porcine liver (≥ 15 units/mg solid), lipase from porcine pancreas (Type II, 100-500 units/mg
209 protein (using olive oil (30 min incubation)), 30-90 units/mg protein (using triacetin)),
210 pancreatin from porcine pancreas (8x USP), pepsin from porcine gastric mucosa (≥ 250
211 units/mg solid) and trypsin from porcine pancreas (lyophilized powder, 1,000-2,000 BAEE
212 units/mg solid) were also purchased from Sigma-Aldrich (Poole, UK).
213
214
215
216
217
218
219
220
221
222
223
224
225

226 227 **2.2 PGA Synthesis**

228 PGA was synthesised following the protocol detailed by Taresco *et al.*[1] Briefly, glycerol
229 (125 mmol) and divinyl adipate (125 mmol) were placed in a three-necked round bottom
230 flask with anhydrous tetrahydrofuran (THF, 50 ml). Novozym 435 (1.1 g) was added and the
231
232
233
234
235
236

237
238
239 resultant mixture stirred at 250 rpm with an overhead stirrer for 24 hours at 50 °C. After this
240 time the immobilised enzyme was removed by filtration and the THF by rotary evaporation.
241
242 The residue was heated at 90 - 95 °C for 1 hour to deactivate any residual enzyme.
243
244

245 **2.3 PGA Modifications**

246
247 PGA-Carboxyfluorescein at two target substitution levels (1% mol/mol & 5% mol/mol, PGA-
248 CF and PGA-CF5, respectively) and PGA-PEG (2% mol/mol substitution) were synthesised
249 using a Steglich Esterification, as previously detailed by Taresco *et al.*[8] This procedure was
250 also used to synthesise PGA-Phe10, PGA-Phe50, PGA-Trp10 and PGA-Trp50; these
251 modifications affect the physicochemical properties of the polymer. Phe refers to
252 phenylalanine, Trp to tryptophan and the number reflects the molar percentage of
253 substitution. The complete reaction scheme for both the production and modification of PGA
254 is shown in Fig. 1. ¹H NMR was used to characterise PGA-CF, PGA-CF5 and PGA-PEG and
255 confirm the couplings were successful; this can be found in Appendix A1-A3 respectively,
256 whereas the characterisation of the amino acid modified polymers has previously been
257 discussed by Taresco *et al.*[8]
258
259
260
261
262
263
264
265

266 *Fig. 1: Synthesis and Modification of PGA.* The reaction scheme for the synthesis of PGA and subsequent
267 modification by Steglich Esterification is shown here. Adapted from Taresco *et al.*[1,8]
268

269 **2.4 Nanoparticle Preparation**

270
271 Nanoparticles were prepared by nanoprecipitation to a final concentration of 1 mg/ml.
272
273 Polymers were dissolved in acetone (1 ml) and added dropwise to ultrapure water under
274 magnetic stirring. The solvent was then allowed to evaporate fully. All nanoparticles had a
275 hydrodynamic diameter between 50-150 nm, measured by DLS (Zetasizer Nano ZS, Malvern
276 Instruments, Malvern, Worcester).
277
278
279

280 **2.5 Dynamic Light Scattering**

281
282 Enzyme solutions (50 µl) were added to nanoparticle suspensions (250 µl) and the change in
283 size over time at 25 °C was measured by DLS. The hydrodynamic diameter of the particles,
284 henceforth referred to as the particle size, was measured at a scattering angle of 173°. Buffer
285 controls, with no enzyme, were also studied to differentiate the effect of the enzyme from that
286 of the buffer. The concentration of the enzyme solution was chosen based on examples from
287 literature, where possible. Where this information was not available several concentrations
288
289
290
291
292
293
294
295

296
297
298 were trialled to find the optimum level. The assay was stopped when the polydispersity
299 exceeded 0.8, insufficient sample remained for accurate measurement or after 6 hours.
300
301

302 The degradation of PGA, PGA-CF and PGA-CF5 was monitored in the presence of elastase
303 and esterase. Analysis of degradation by elastase was carried out in both Tris buffer (0.1 mM,
304 pH 8.0) and Hepes buffer (0.5 M, pH 6.5). The enzyme solution was at a concentration of
305 1.74 units/ml, assessed using the method provided by Sigma-Aldrich, [Appendix B.1
306 Elastase] whereby one unit of elastase is defined as the amount that will hydrolyse 1.0 μ mole
307 of N-succinyl-L-Ala-Ala-Ala-p-nitroanilide per minute at pH 8.0 at 25 °C in Tris buffer (0.1
308 mM).[24] For the experiments with esterase 75.3 units/ml of enzyme in borate buffer (10
309 mM, pH 8.0) and 225.9 units/ml in phosphate buffered saline (PBS, pH 7.4) were used as the
310 enzyme solutions. Activity was assessed using a method available from Sigma-Aldrich,
311 [Appendix B.2 Esterase] with one unit defined as the amount that will hydrolyse 1.0 μ mole of
312 ethyl butyrate to butyric acid and ethanol per minute at pH 8.0 at 25 °C in borate buffer (10
313 mM).[25]
314
315
316
317
318
319
320
321

322 The degradation of PGA, PGA-PEG, PGA-Phe10 & 50 and PGA-Trp10 & 50 in the presence
323 of lipase, pancreatin, pepsin and trypsin was studied. Lipase was prepared in PBS (pH 7.4) to
324 a concentration of 10 mg/ml (215.4 units/ml). The novel method used for determining lipase
325 activity can be found in Appendix B.3 Lipase; one unit was defined as the amount required to
326 cleave 1.0 nmole of 4-methylumbelliferyl butyrate (4-MUB) per minute in Tris buffer (pH 7.5,
327 0.2 M) at room temperature and with a total reaction volume of 3 ml. The amount of 4-MUB
328 cleaved was calculated using a calibration curve of the fluorescence intensity of the product,
329 4-methylumbelliferone [Appendix B.3 Lipase, Fig. B.4]. Pancreatin was prepared in
330 Simulated Intestinal Fluid (pH 7.5) according to United States Pharmacopeia (USP)
331 specifications. Pepsin was prepared in Simulated Gastric Fluid (pH 1.2) according to USP
332 specifications. For the experiments with trypsin, 15582 units/ml of enzyme in sodium
333 phosphate buffer (1 mM, pH 7.6) was used as the enzyme solution. Trypsin activity was
334 determined using a method available from Sigma-Aldrich, [Appendix B.4 Trypsin] and one
335 unit was defined as the amount required to produce a change in absorbance at 253 nm of
336 0.001 per minute with N α -Benzoyl-L-arginine ethyl ester as the substrate with sodium
337 phosphate monobasic buffer (67 mM, pH 7.6) at 25 °C in a reaction volume of 3.20 ml.[26]
338
339
340
341
342
343
344
345
346
347
348
349
350
351
352
353
354

2.6 Release of Carboxyfluorescein by Dialysis

Regenerated Cellulose Dialysis Tubing with a 3.5 kDa MWCO (Type T1, Fisherbrand, Loughborough, UK) was washed in sterile water and stored in 0.1% sodium benzoate at 4 °C until use. The preparation and filling of the dialysis membranes took place in a Class II cabinet to minimise microbial contamination. Nanoparticles and buffer solutions were passed through a 0.22 µm filter before use.

PGA-CF5 nanoparticles (2 ml, 1 mg/ml) were placed in dialysis membranes along with enzyme solution and/or buffer up to a final volume of 5 ml. This was placed in buffer (195 ml) and incubated at 37 °C in a shaking water bath. Samples were periodically removed and replaced with fresh buffer. Further aliquots of enzyme were added at 3, 6, 24, 48 and 72 hours to maintain enzyme activity. Blank experiments were carried out with each buffer with no enzyme present to differentiate between hydrolytic and enzymatic degradation. Fluorescence Intensity was measured in triplicate at an excitation wavelength of 492 nm and an emission wavelength of 517 nm using a Cary Eclipse Fluorescence Spectrophotometer (Agilent Technologies, Santa Clara, CA). Calibration curves of carboxyfluorescein in each buffer were produced and used to calculate the concentration in each sample. This concentration was used to calculate the cumulative percentage molar release of carboxyfluorescein over time.

The effect of three enzymes, lipase, esterase and elastase, was studied. The amount of enzyme used here, and for each of the remaining experiments, was equivalent to that which was used in the DLS experiments, scaled up relative to the amount of polymer used. The lipase experiments were carried out in phosphate buffered saline (PBS) at pH 7.4 with 4 mg lipase used for each enzyme addition. Borate buffer (10 mM, pH 8.0) was used as the buffer with esterase, with 33 units of esterase used for each enzyme addition. For the elastase experiments 0.82 units were used for each enzyme addition, and Hepes buffer (0.1 M) was used at pH 6.5.

2.7 Characterisation of Degraded Polymer

The degradation of PGA-CF5 in the presence of lipase, esterase and elastase was characterised by GPC, FTIR and ¹H NMR. The same incubation conditions and pattern of enzyme addition as in the release experiments were used. The ratio of polymer to enzyme

414 was maintained, however, the amount of polymer used was increased to facilitate analysis.
415
416 Three incubation times, ranging from 24 - 96 hours, were used for GPC analysis and for the
417
418 sample incubated with lipase analysed by NMR and FTIR. The esterase and elastase samples
419
420 for NMR and FTIR analysis were incubated for 96 hours. After incubation samples were
421
422 freeze-dried (Sentry 2.0, Virtis SP Scientific, Gardiner, NY) to remove the buffer.
423
424

425 Gel Permeation Chromatography (GPC, PL50, Polymer Laboratories, Salop, UK) was carried
426
427 out using dimethylformamide (DMF) + 0.1% LiBr as the mobile phase at a flow rate of 1
428
429 ml/min. Two mixed bed D columns were employed, kept at a constant temperature of 50 °C.
430
431 Poly(methyl methacrylate) standards (M_n range 1,810,000 – 505 g mol⁻¹) were used to
432
433 calibrate the size-exclusion chromatography system. The enzyme was precipitated with
434
435 acetone (3 ml per sample) prior to analysis. In addition to the enzyme samples, controls were
436
437 carried out using untreated PGA-CF5 and polymer which had been incubated at 37 °C
438
439 without enzyme present to allow accurate interpretation of the effect of the enzymes.

439 FT-IR spectra were recorded with an Attenuated Total Reflection Cary 630 FTIR
440
441 spectrophotometer (Agilent Technologies, Santa Clara, CA). 128 interferograms were
442
443 recorded for each spectrum in the range 4000-650 cm⁻¹.
444

445 ¹H NMR spectra were recorded using acetone-d₆ and deuterium oxide on a Bruker 400 MHz
446
447 spectrophotometer (Billerica, MA). Chemical shifts were reported as parts per million (δ)
448
449 downfield from an internal standard, tetramethylsilane. Acetone (1 ml per sample, unless
450
451 stated) was used to precipitate the enzyme before analysis.

452 **2.8 Statistical Analysis**

453

454 Two-way ANOVA was performed on the results for the release of carboxyfluorescein in
455
456 order to determine statistical significance. The percentage carboxyfluorescein release in the
457
458 presence of each enzyme was compared with the relevant buffer without enzyme present.
459
460 Following this f-tests were used to determine if the variance of the groups was significantly
461
462 different. This information was used to select the appropriate two tailed unpaired t-test for
463
464 each enzyme and buffer pair. A t-test was carried out at each time point to ascertain when
465
466 there was a significant difference in release with and without enzyme present, with
467
468 significance set at a p-value of 0.05.
469

3. Results

3.1 Change in Particle Size by Dynamic Light Scattering

DLS was used as a rapid screening technique, monitoring the change in nanoparticle size and polydispersity following the addition of a small aliquot of enzyme. The purpose of these experiments was to gain an insight into how the polymeric nanoparticles may behave *in vivo* and to select appropriate conditions for future experiments. This experiment was intended to provide a binary prediction of whether or not a particular enzyme would degrade a particular polymer, rather than a quantitative measure of that degradation. It has been suggested that the increase in particle size represents swelling, followed by the collapse of the particle, which can be taken as an indication of degradation.[27]

3.1.1 Comparison of Different Enzymes

The effect of each of the different enzymes on PGA nanoparticles was studied to facilitate comparison. Additionally, two buffers were used with both esterase and elastase in order to explore the impact of pH. Together with buffers reflecting the optimum pH for activity, esterase was studied at pH 7.4 to reflect the environment of the blood and elastase was studied at pH 6.5. In the 1920s Warburg *et al.*[28,29] discovered that the tumour microenvironment tends to have a slightly acidic pH, consequently, understanding the effect of lowering the pH may be beneficial for future applications of this polymer in cancer drug delivery.

Simulated gastric fluid caused an increase in particle size exceeding that seen with pepsin. This is likely to be a result of the acidic pH of this buffer, 1.2, at which the nanoparticles do not appear to be stable. Consequently, the remainder of the results presented here exclude pepsin. The effect of the buffer was found to be negligible for all of the other conditions studied.

A dramatic change in PGA nanoparticle size was seen with lipase, pancreatin and elastase in HEPES buffer, suggesting degradation was occurring. A change in nanoparticle size was also seen with elastase in Tris buffer [Fig 2]. The effect seen with trypsin was limited, with a small change in size in the region of 100 nm. Additionally, the effect of esterase on particle size was limited in borate buffer (pH 8) and in PBS (pH 7.4).

3.1.2 Comparison of Different Polymer Modifications

Nanoparticles made using modified PGA were tested with each of the enzymes to investigate the effect of these structural changes on the extent of degradation. These modifications were the addition of PEG to the end of the polymer chain and the conjugation of carboxyfluorescein, at 2% & 5%, or the amino acids phenylalanine and tryptophan, at 10% and 50%, to the pendant hydroxyl group of the polymer backbone. The modified polymers were compared with the unmodified PGA.

Interestingly, differences were observed between polymer modifications incubated with the same enzyme. For lipase, pancreatin and trypsin the change in size of PGA-PEG nanoparticles was an order of magnitude less than that seen for the unmodified PGA [Fig. 2]. The effect of the other modifications was less consistent. A change in size was seen for PGA and the carboxyfluorescein modified polymers upon incubation with elastase, with the extent of this change differing depending on the level of carboxyfluorescein modification. With esterase in both buffers there was no size change seen at all for the carboxyfluorescein modified polymers, and a limited effect on the size of PGA nanoparticles, meaning the differences between polymers may not be significant. For lipase and pancreatin the amino acid modifications appeared to reduce the effect of the enzymes, yet for trypsin the opposite was true. Furthermore, for all polymers with trypsin it took some time before any change in size was seen.

Fig. 2: Effect of Backbone Modifications on PGA Degradation. The colour of each bar here reflects the polymer under investigation. The results for pepsin have been omitted as it was not possible to differentiate the effect of the enzyme from that of the buffer.

3.2 Release of Coupled Carboxyfluorescein

PGA-CF5 was used here as a model of a low loading of drug coupled to PGA, allowing the release of carboxyfluorescein from the polymer to be monitored over time. This was to provide an indication of the way a drug would be released if coupled to the polymer backbone.

Lipase was seen to significantly increase the release of carboxyfluorescein in comparison with the buffer alone [Fig. 3A]. Two-way ANOVA analysis suggested this difference was highly significant with a p-value of <0.0001. Furthermore, studying each time point individually suggested a significant difference between the release of carboxyfluorescein with

591
592
593 and without lipase present from 2 hours onwards. After 96 hours the release of
594 carboxyfluorescein in the presence of lipase was calculated as 23% whereas in PBS alone it
595 was 7%. Several distinct phases could be identified in the release of the carboxyfluorescein.
596 There was an initial burst release over the first few hours; this is thought to be due to the ester
597 bonds of carboxyfluorescein present in the surface layers of the nanoparticles being easily
598 accessible to the enzyme and so rapidly cleaved, releasing the dye. Following this there was a
599 more gradual release of the internal carboxyfluorescein before approaching a plateau from 24
600 hours onwards. The release was not calculated to be 100%, however, no carboxyfluorescein
601 could be detected within the dialysis membrane, suggesting a spectral shift may be occurring
602 which reduces the apparent concentration of carboxyfluorescein. The release seen here is
603 typical for many polymeric nanoparticle formulations.[30]
604
605
606
607
608
609
610

611
612 The experiments investigating the effect of elastase were carried out in the presence of HEPES
613 buffer at pH 6.5. These conditions were chosen as pH 6.5 saw a larger particle size increase
614 by DLS than pH 8.0. Elastase caused a significant increase in carboxyfluorescein release
615 when compared with the buffer alone from 48 hours onwards, with p-values < 0.05. The
616 release was calculated as 5.6% with the buffer alone and 9.6% in the presence of elastase
617 after 96 hours; this increase was less than that seen with lipase [Fig. 3B].
618
619
620
621

622
623 Since the DLS results for esterase at both pH values failed to show an effect, borate buffer
624 (pH 8.0) was preferred for these experiments as it represents the optimum conditions for
625 esterase action. The release of carboxyfluorescein was calculated to be 5.8% in the presence
626 of esterase after 96 hours, compared with 1.8% with the borate buffer alone. Overall, this
627 difference was not found to be significant. Examining each time point individually, there was
628 a significant difference in the release at 6 hours (p-value = 0.005), however, this difference
629 was not maintained. Furthermore, a high level of variability between samples was observed
630 [Fig. 3C]. Any increase in release seen with esterase is, therefore, likely to be a result of
631 hydrolytic degradation.
632
633
634
635
636
637

638 *Fig.3 A-C: Release of Carboxyfluorescein in the Presence of Lipase, Elastase and Esterase.* The release of
639 carboxyfluorescein in the presence of lipase, elastase and esterase is shown in A, B & C, respectively and each
640 graph also shows the relevant buffer control. The points used here are the average of three experiments whereas
641 the error bars represent 1 standard deviation. Calculated p-values for each time point, comparing release with
642 and without the enzyme are indicated by asterisks.
643
644
645
646
647
648
649

3.3 Change in Polymer Molecular Weight Following Incubation with Enzymes

The release of carboxyfluorescein detailed in the previous section strongly suggests the polymer was breaking down in the presence of enzymes. In order to analyse this in a quantitative manner, GPC was used to monitor the effect of incubation with enzymes on the molecular weight of PGA-CF5. The chromatographs and distribution plots generated for each sample can be found in the Supplementary Information [Appendix C].

Where no enzyme was present there was relatively little change in the GPC traces compared with the untreated sample, suggesting PGA was stable at 37 °C for the duration of the time period studied [Fig. 4A].

Upon incubation with lipase, a dramatic decrease in molecular weight was observed at 24 hours, with a similar result seen for the remaining time points [Fig. 4]. The peak representing the intact polymer as seen in the untreated sample was absent, suggesting no polymer remained. Only small molecular fragments were detected, however these could not be quantified as they approached the calibration limit of the instrument and the solvent peak.

At each studied time point two peaks were detected for those samples incubated with elastase; the first of these peaks represents a size consistent with untreated polymer whereas the second represents small breakdown products [Fig. 4]. Interestingly, with increasing incubation time, the size of the peak representing the intact polymer decreased relative to the peak of the small breakdown products. This suggests partial degradation occurs with elastase, with the amount of intact polymer decreasing over time as the degradation progresses.

The change seen following incubation with esterase was less dramatic than that observed with lipase and elastase, with a limited change in molecular weight [Fig. 4A]. However, the range of molecular weights appeared to narrow and the polydispersity (\mathcal{D}) decreased relative to the untreated sample [Fig. 4B]. This change indicates the loss of small fractions from the end of the larger polymer chains, rather than breakages from the centre of the chain.

The GPC analysis confirms that PGA-CF5 is entirely broken down in the presence of lipase, with no intact polymer chains remaining. Degradation also occurs to a lesser extent in the presence of elastase, with both degraded and intact chains present in each sample. Finally,

709
710
711 there is a change in the size distribution of PGA-CF5 incubated with esterase, suggesting
712 minimal degradation is occurring.
713
714

715 *Fig. 4 A & B: GPC Traces, Molecular Weight and Polydispersity of PGA-CF5 Following Enzyme Incubation.*
716 In A the traces for each sample are presented, grouped by enzyme. The large peaks seen in the region of 1000
717 seconds represent the eluent. There is little difference between the untreated sample and the blank samples,
718 incubated without enzyme, suggesting the changes seen upon incubation with enzymes are as a result of
719 enzymatic degradation. In B the number average molecular weight (M_n) and Polydispersity (D) are listed.
720

721 **3.4 Changes to Chemical Structure of PGA Following Enzyme** 722 **Incubation** 723

724 The changes to the structure of PGA following the addition of enzymes was investigated in
725 order to confirm breakdown was occurring and to understand the spectral changes seen with
726 the released carboxyfluorescein.
727
728

729 **3.4.1 FTIR** 730

731 FTIR was used to provide a rapid indication of whether degradation had occurred. Several
732 differences can be seen between the spectra of PGA-CF5 alone and those of the polymer
733 incubated with lipase. The OH stretch between $3500-3000\text{ cm}^{-1}$ shifts to lower wavelengths
734 with time, indicative of the presence of carboxylic acid groups, increased hydrogen bonding
735 and the formation of dimers [Fig. 5A, peak I]. The peak representing the C=O ester bond at
736 1750 cm^{-1} , visible in the untreated sample, is not seen from 72 hours of incubation with lipase
737 onwards. Instead, there is a broad area of peaks between $1700-1500\text{ cm}^{-1}$, representing
738 overlapping vibrations from a range of different C=O carboxyl bonds [Fig 5A, peak II].
739 Finally, there are new peaks visible in the region of the spectra below 1000 cm^{-1} which are
740 not seen with the untreated PGA-CF5; these peaks represent changes to the environment of
741 the aromatic ring structure of carboxyfluorescein [Fig. 5A, peak III]. These changes to the
742 FTIR spectra appear likely to show the breakdown of the ester bond, and subsequently the
743 polymer, on incubation with lipase.
744
745
746
747
748
749
750
751
752

753
754 PGA-CF5 incubated with elastase, the untreated polymer and the enzyme alone were
755 analysed by FTIR and the spectra compared; two main areas of difference were identified. As
756 with the lipase samples, the peak at 1750 cm^{-1} [Fig. 5B, peak I], representing the C=O of the
757 ester bond, reduced in intensity between the untreated and treated samples, suggesting a
758 proportion of these bonds were broken. Additionally, three peaks appeared at 990, 1030 &
759
760
761
762
763
764
765
766
767

768
769
770 1160 cm⁻¹ [Fig. 5B, peak II] in the sample incubated with enzyme, representing a C-O
771 alcohol bond forming in place of the ester bond.
772

773
774 PGA-CF5 incubated with esterase, untreated PGA-CF5 and esterase alone were analysed by
775 FTIR and the spectra compared to ascertain the effect of the enzyme. The enzyme alone
776 produced two clear peaks at 1530 & 1640 cm⁻¹ [Fig. 5C, peak III] which can also be seen for
777 the incubated sample. The main difference between the spectra of the treated and untreated
778 PGA-CF5 is the OH stretching area at 3500-3000 cm⁻¹, the OH stretching area where the
779 typical broad peak representative of alcohols, seen in the untreated sample, is replaced by a
780 sharp acidic peak due to the formation of dimers [Fig. 5C, peak I]. Additionally, the peak at
781 1720 cm⁻¹ [Fig. 5C, peak II], resulting from the C=O ester bond, disappears following
782 incubation with the enzyme, providing further suggestion of breakdown.
783
784
785
786
787
788
789

790 *Fig. 5 A-C: FTIR Spectra of PGA-CF5 Before and After Incubation with Enzymes.* Incubation with lipase is
791 shown in A, elastase in B and esterase in C. The key differences in the spectra are highlighted with blue boxes
792 and the peak allocation is discussed in the text. In all cases the spectrum for untreated PGA-CF5 is shown in
793 black. For lipase (A) PGA-CF5 after 24 hours incubation with lipase is in red; 72 hours incubation is in green
794 and 96 hours incubation is in dark blue. Lipase alone is shown in sky blue. For elastase and esterase (B & C),
795 PGA-CF5 incubated with the respective enzyme is shown in red and the enzyme alone is shown in green.
796

796 3.4.2 ¹H NMR

797
798 ¹H NMR was used to provide a more detailed examination of the structural changes following
799 incubation with the enzymes. Analysis was carried out in acetone-d₆ and deuterium oxide.
800 Any remaining polymer would be visible in the acetone but would not be present in the
801 deuterium oxide, whereas the degradation products would be soluble in both acetone and
802 deuterium oxide. Consequently, this allowed the degradation products to be identified more
803 easily in deuterium oxide in the absence of the intact polymer peaks. Allocation of the peaks
804 corresponding to PGA has been discussed previously in detail by Taresco *et al.*[1]
805
806
807
808
809

810 Following incubation with lipase, it was possible to observe peaks corresponding to
811 carboxyfluorescein (6.5-8.0 ppm), glycerol (3.5-4.0 ppm), adipic acid (1.3 ppm) and the
812 intact polymer (1.6, 2.3, 4.0 ppm) in acetone-d₆ [Figs. 6 A & B]. Furthermore, a mixture of
813 breakdown products could be observed in the region of 4.75-5.5 ppm, with peaks
814 corresponding to a dimer of the repetitive unit of PGA and carboxyfluorescein coupled to one
815 PGA monomer unit. This suggests that the breakdown is not always complete.
816
817
818
819
820
821
822
823
824
825
826

827
828
829 When analysed in deuterium oxide the peaks representing adipic acid (0.5-2.5 ppm) remain
830 visible; there are many peaks suggesting a range of variations are present [Figs. 6 A & C]. It
831 was possible to study the glycerol present in more detail; as well as free glycerol (3.6, 3.7,
832 3.9, 5.1 ppm) there is also a conjugate of glycerol and carboxyfluorescein (4.4 ppm).
833
834 Additionally, the peak labelled j (8.0-8.3 ppm), which represents the proton adjacent to the
835 ester bond of carboxyfluorescein, shifts with increasing incubation time as the environment
836 changes, confirming the breakdown of this bond.
837
838

839
840
841 The NMR spectra of PGA-CF5 incubated with elastase, recorded in acetone-d₆ and deuterium
842 oxide, do not differ significantly from those seen with lipase. The same breakdown products
843 can be observed, with the polymer breaking down both partially and fully. As a result of this
844 similarity the data is not presented here.
845
846
847

848
849 As with the lipase and elastase samples, esterase was precipitated from the incubated sample
850 before ¹H-NMR analysis in acetone-d₆ and deuterium oxide. It proved difficult to precipitate
851 the enzyme from the sample following freeze drying; a large amount of acetone was required
852 and the enzyme was seen to be yellow in colour, suggesting carboxyfluorescein remained
853 within the precipitate. The spectrum obtained when analysing the incubated sample in
854 acetone-d₆ appeared to be broadly similar to the spectra obtained for the lipase and elastase
855 samples, albeit with less clarity [Fig. 6D]. The peaks for the polymer, adipic acid, glycerol
856 and carboxyfluorescein remained visible. Again, breakdown products could be seen in the
857 region of 5.0-5.5 ppm, however, there was no peak visible at 4.75 ppm as was seen for lipase
858 [Fig. 6A, peak q]. This peak represents the proton adjacent to the secondary alcohol of
859 glycerol found in the dimer [Fig. 6A]. The presence of a peak at 5.3 ppm suggests the dimer
860 is produced, however, it is likely to be in a small amount. Otherwise, the same breakdown
861 products were as seen with lipase and elastase.
862
863
864
865
866
867
868
869

870
871 When analysed in deuterium oxide, the spectrum for PGA-CF5 incubated with esterase
872 lacked definition. Areas of the spectrum relating to carboxyfluorescein, glycerol and adipic
873 acid could be identified, however, it was not possible to allocate specific peaks.
874
875 Consequently, this spectrum has not been displayed here. This is likely to be a result of the
876 difficulty precipitating the enzyme, however, this precipitation was essential to gain any level
877 of spectral clarity.
878
879
880
881
882

886
887
888
889 *Fig. 6 A-D: NMR Spectra of PGA-CF5 Incubated with Enzymes and Corresponding Labelled Structures:* The
890 labelled structures shown in A correspond with each of the following spectra examining degradation by lipase,
891 elastase and esterase in acetone-d₆ and deuterium oxide. The spectrum in B is PGA-CF5 after incubation for 24
892 hours in lipase, analysed in acetone-d₆. The spectra for 72 & 96 hours were very similar, and so are not shown
893 here. In C analysis was carried out in deuterium oxide. The top spectrum is after 24 hours of incubation with
894 lipase, the middle spectrum after 72 hours and the bottom spectrum after 96 hours. The spectrum in D is PGA-
895 CF5 following incubation with esterase, analysed in acetone-d₆. The key difference between this spectrum and
896 those for elastase and lipase is the absence of one peak from the area labelled 'Polymer Breakdown Products'.

897 898 **4. Discussion**

899
900 DLS showed that the size of PGA nanoparticles increases after the addition of a range of
901 enzymes, with the extent of this change differing depending on the enzyme and polymer
902 modifications. Lipase and elastase were found to significantly increase the release of
903 carboxyfluorescein, compared with buffer alone. The calculated release remained below
904 100%, however, the presence of carboxyfluorescein-monomer and carboxyfluorescein-
905 glycerol conjugates, identified by NMR, in the polymer degradation products may provide an
906 explanation for the observed spectral shift, and consequent underestimation of release. NMR,
907 FTIR and GPC were also used to confirm the breakdown of the polymer in the presence of
908 lipase, elastase and esterase; complete breakdown was seen with lipase whereas partial
909 breakdown could be seen with the other two enzymes.
910
911

912
913
914
915
916 DLS was used here as a rapid screening method. The limitation of using DLS to explore
917 enzyme degradation in more detail is that it can be difficult to understand exactly what is
918 changing and why. Certainly, the fact that after a point it becomes impossible to gain
919 meaningful results would support this hypothesis. Furthermore, in this study it was noted that
920 the attenuator number, automatically selected by the Zetasizer ZS to provide the best
921 measurements, increased over time. For example, the addition of elastase in Tris buffer to
922 PGA nanoparticles caused the attenuator number to increase from 5 to 8, suggesting the
923 concentration of nanoparticles in the sample was decreasing. It must also be noted that
924 Malvern Panalytical suggest a maximum particle size of 10 µm, sample dependant, for the
925 Zetasizer ZS [31] and the sizes seen here are approaching that point. Consequently, small
926 nanometre size differences in the micrometre size range may be artefacts of the technique.
927
928
929
930

931
932
933
934
935 The results seen here strongly suggest PGA nanoparticles are susceptible to degradation by a
936 number of enzymes and that modifications of the polymer backbone can influence this
937 degradation. Further investigations were, however, required to provide a better understanding
938
939
940
941

945
946
947 of this. As the breakdown of the polymer and the release of any drug was considered to be
948 more relevant from a drug delivery perspective than changes in particle morphology,
949 analytical techniques were preferred to imaging techniques.
950
951

952
953 Generally, aliphatic polyesters with a short chain between ester groups, such as PGA, are
954 found to undergo hydrolysis in a biologically relevant time frame.[9] The use of lipase in the
955 synthesis of the polymer shows it is a viable substrate and so suggests PGA will be
956 degradable by this enzyme. These features are also found in poly(caprolactone) (PCL) which
957 can be synthesised by enzymatic ring opening polymerisation using lipase. This polymer
958 features 5 carbons between the ester groups, however, PCL is not enzymatically degraded *in*
959 *vivo*. [32] This may be as a result of the thermal properties; PCL is solid at both room
960 temperature and 37 °C due to its crystalline nature, [32] and consequently access of the
961 enzyme catalytic site to the ester group may be restricted. Conversely, PGA is a viscous
962 liquid at 37 °C, [1] and this more fluid nature can be expected to allow easier access of the
963 enzyme, suggesting why enzymatic degradation may be observed with PGA and not with
964 PCL. These structural features and physical properties, combined with the use of enzymatic
965 synthesis, indicate PGA may be similarly susceptible to degradation by other hydrolases to a
966 greater extent than traditional polyesters.
967
968
969
970
971
972
973
974
975

976
977 The DLS results gathered here suggest modifying the polymer backbone affects the
978 susceptibility of PGA to enzymatic degradation. In the presence of lipase, pancreatin and
979 trypsin PGA-PEG nanoparticles demonstrated a smaller change in size compared with
980 unmodified PGA. This suggests PEG provides a protective role by forming a corona on the
981 surface of the particles, sterically hindering enzyme access. [33] PGA-PEG could, therefore,
982 be adopted should a slower breakdown and release profile be desired. With lipase and
983 pancreatin the amino acid modifications appeared to reduce the effect of the enzymes. These
984 modifications would be expected to increase the stability of the particles as a result of π - π
985 stacking of the aromatic rings. [8] This was not seen with trypsin and may be because trypsin
986 is a protease with high specificity for arginine and lysine residues, [34] rather than the ester
987 bonds found in PGA.
988
989
990
991
992
993
994

995
996 The active site of porcine pancreatic lipase (PPL) comprises a catalytic triad, with lid domain
997 loops providing steric hindrance. However, in aqueous environments hydrogen bonds
998 between the lid and co-lipase tend to stabilise it in an open conformation, allowing substrate
999
1000

1004
1005
1006 access,[35] and in this case the breakdown of PGA. Furthermore, the natural substrates of
1007
1008 PPL are glycerol esters, which would explain why it works effectively on PGA resulting in
1009
1010 the structural changes observed by NMR and FTIR and the absence of intact polymer by
1011
1012 GPC. Pancreatin is a mixed enzyme preparation containing lipase, trypsin, amylase,
1013
1014 ribonuclease and protease. Consequently, the effect of pancreatin would be expected to be a
1015
1016 summation of the contribution of each of these enzymes, meaning the degradation of PGA by
1017
1018 pancreatin would be expected to equal or exceed that seen with lipase alone.

1018
1019 Porcine pancreatic elastase (PPE) is a serine protease with broad specificity[36] and
1020
1021 crystalline PPE has been reported to have a relatively open active site.[37] While the
1022
1023 specificity of elastase is generally discussed in terms of peptides, this open site and the noted
1024
1025 broad specificity may suggest a reason why release was seen with this particular enzyme
1026
1027 preparation. While breakdown is evident by NMR, FTIR and GPC, the results were less clear
1028
1029 than those seen with lipase. This may be as a result of the reduced specificity of the enzyme,
1030
1031 when compared with lipase, resulting in partial degradation. This finding is in agreement with
1032
1033 the lower release of carboxyfluorescein and the presence of intact polymer following GC
1034
1035 analysis of PGA-CF5 incubated with elastase.

1034
1035 The active site of esterase has been reported to be highly constrained as a result of the
1036
1037 surrounding amino acids. The Jones Cubic Space model has been used to predict whether or
1038
1039 not a molecule will be a substrate for carboxyesterase.[38] Carboxyfluorescein, PGA and
1040
1041 PGA-CF5 are much larger than the active site defined by this model, and as a result would
1042
1043 not be expected to be substrates for esterase. This suggests a reason why carboxyfluorescein
1044
1045 release is limited and also why a high degree of variability was observed. Whilst there is clear
1046
1047 evidence by NMR and FTIR that PGA-CF5 undergoes degradation in the presence of
1048
1049 esterase, it was more difficult to ascertain the structure of the breakdown products than was
1050
1051 the case with PGA-CF5 incubated with either lipase or elastase. The low level of
1052
1053 carboxyfluorescein release, along with the constrained nature of the active site of the enzyme,
1054
1055 means this difficulty was not unexpected. Furthermore, the small changes in molecular
1056
1057 weight seen when PGA-CF5 was incubated with esterase, suggesting breakdown at the end of
1058
1059 the polymer chains, would concur with the theory regarding the constrained nature of the
1060
1061 active site of esterase,[38] as the steric hindrance would be greatly reduced at the chain ends.
1062

1063
1064
1065
1066
1067
1068
1069
1070
1071
1072
1073
1074
1075
1076
1077
1078
1079
1080
1081
1082
1083
1084
1085
1086
1087
1088
1089
1090
1091
1092
1093
1094
1095
1096
1097
1098
1099
1100
1101
1102
1103
1104
1105
1106
1107
1108
1109
1110
1111
1112
1113
1114
1115
1116
1117
1118
1119
1120
1121

In general terms the breakdown of PGA seen here is of clinical importance as it suggests breakdown would also be observed *in vivo*. This is crucial from a safety point of view and justifies the label ‘biodegradable’. Furthermore, this breakdown, coupled with the effective release of coupled carboxyfluorescein suggests PGA would be viable as a drug delivery platform as active drug molecules could be expected to be released in a similar controlled manner. The differences seen with the various backbone modifications suggest the potential for tunable degradation which may be exploited for controlled release. Furthermore, the variable degradation and release seen with different enzymes could be used for targeting purposes; release can be expected to be higher in areas with high concentrations of lipase than where other enzymes prevail. The susceptibility of PGA to gastro-intestinal enzymes also opens the possibility for using the polymer for oral drug delivery in the future.

5. Conclusion

Pancreatin, lipase, elastase and trypsin were all found to cause a change in the size of PGA nanoparticles, indicative of degradation. Modifications of the polymer backbone altered the degree of size change seen; the effect was particularly pronounced for PGA-PEG, which consistently showed decreased degradation relative to unmodified PGA. Lipase, elastase and esterase were shown to increase the release of coupled carboxyfluorescein from the polymer; this increase was statistically significant with lipase and elastase. GPC analysis of the molecular weight of PGA-CF5 following incubation with lipase, elastase and esterase, provided evidence of polymer breakdown while illustrating the importance of the specificity of the enzymes on the extent of the degradation. Lipase was found to cause complete breakdown of PGA-CF5 by 24 hours, whereas elastase caused partial breakdown and the effect of esterase was limited. The structure of PGA-CF5 incubated with lipase, elastase and esterase was analysed to understand the way in which the polymer was breaking down. The breakdown of the ester bond in the PGA backbone could be seen along with the release of carboxyfluorescein, a carboxyfluorescein-monomer conjugate and a dimer of PGA.

Taken together, these data demonstrate the high enzymatic degradability of PGA based polymers into non-toxic building blocks by a range of relevant enzymes. Interestingly, a low level of PEGylation or varying the nature of the free hydroxyl group in the polymer backbone by conjugation with amino acids has been shown to affect the susceptibility of the polymer to degradation. This phenomenon may be exploited to tune the degradation of PGA for specific

1122
1123
1124
1125
1126
1127
1128
1129
1130
1131
1132
1133
1134
1135
1136
1137
1138
1139
1140
1141
1142
1143
1144
1145
1146
1147
1148
1149
1150
1151
1152
1153
1154
1155
1156
1157
1158
1159
1160
1161
1162
1163
1164
1165
1166
1167
1168
1169
1170
1171
1172
1173
1174
1175
1176
1177
1178
1179
1180

pharmaceutical or biomedical applications in order to achieve controlled release rates and breakdown profiles, thereby optimising dosage regimens and patient adherence.

6. Acknowledgements

This work was funded and supported by the Centre for Doctoral Training in Advanced Therapeutics and Nanomedicines (School of Pharmacy, University of Nottingham), Pfizer Ltd. and the Engineering and Physical Sciences Research Council (EPSRC), Grant Numbers: EP/L01646X and EP/N03371X/1.

7. References

- [1] V. Taresco, R.G. Creasey, J. Kennon, G. Mantovani, C. Alexander, J.C. Burley, M.C. Garnett, Variation in structure and properties of poly(glycerol adipate) via control of chain branching during enzymatic synthesis, *Polymer (Guildf)*. 89 (2016) 41–49. doi:10.1016/j.polymer.2016.02.036.
- [2] T. Naolou, V.M. Weiss, D. Conrad, K. Busse, K. Mäder, J. Kressler, Fatty acid modified poly(glycerol adipate) -Polymeric analogues of glycerides, in: *ACS Symp. Ser.*, 2013: pp. 39–52. doi:10.1021/bk-2013-1135.ch004.
- [3] C. Korupp, R. Weberskirch, J.J. Müller, A. Liese, L. Hilterhaus, Scaleup of lipase-catalyzed polyester synthesis, *Org. Process Res. Dev.* 14 (2010) 1118–1124. doi:10.1021/op1000868.
- [4] L.E. Iglesias, Y. Fukuyama, H. Nonami, R. Erra-Balsells, A. Baldessari, A simple enzymatic procedure for the synthesis of a hydroxylated polyester from glycerol and adipic acid, *Biotechnol. Tech.* 13 (1999) 923–926. doi:10.1023/A:1008958212814.
- [5] V.M. Weiss, T. Naolou, G. Hause, J. Kuntsche, J. Kressler, K. Mäder, Poly(glycerol adipate)-fatty acid esters as versatile nanocarriers: From nanocubes over ellipsoids to nanospheres, *J. Control. Release.* 158 (2012) 156–164. doi:10.1016/J.JCONREL.2011.09.077.
- [6] P. Kallinteri, S. Higgins, G.A. Hutcheon, C.B. St. Pourçain, M.C. Garnett, Novel functionalized biodegradable polymers for nanoparticle drug delivery systems, *Biomacromolecules.* 6 (2005) 1885–1894. doi:10.1021/bm049200j.
- [7] V.M. Weiss, T. Naolou, T. Groth, J. Kressler, K. Mäder, In vitro toxicity of stearyl-poly(glycerol adipate) nanoparticles, *J. Appl. Biomater. Funct. Mater.* 10 (2012) 163–169. doi:10.5301/JABFM.2012.10294.
- [8] V. Taresco, J. Suksiriworapong, I.D. Styliari, R.H. Argent, S.M.E. Swainson, J. Booth, E. Turpin, C.A. Laughton, J.C. Burley, C. Alexander, M.C. Garnett, New N-acyl amino acid-functionalized biodegradable polyesters for pharmaceutical and biomedical

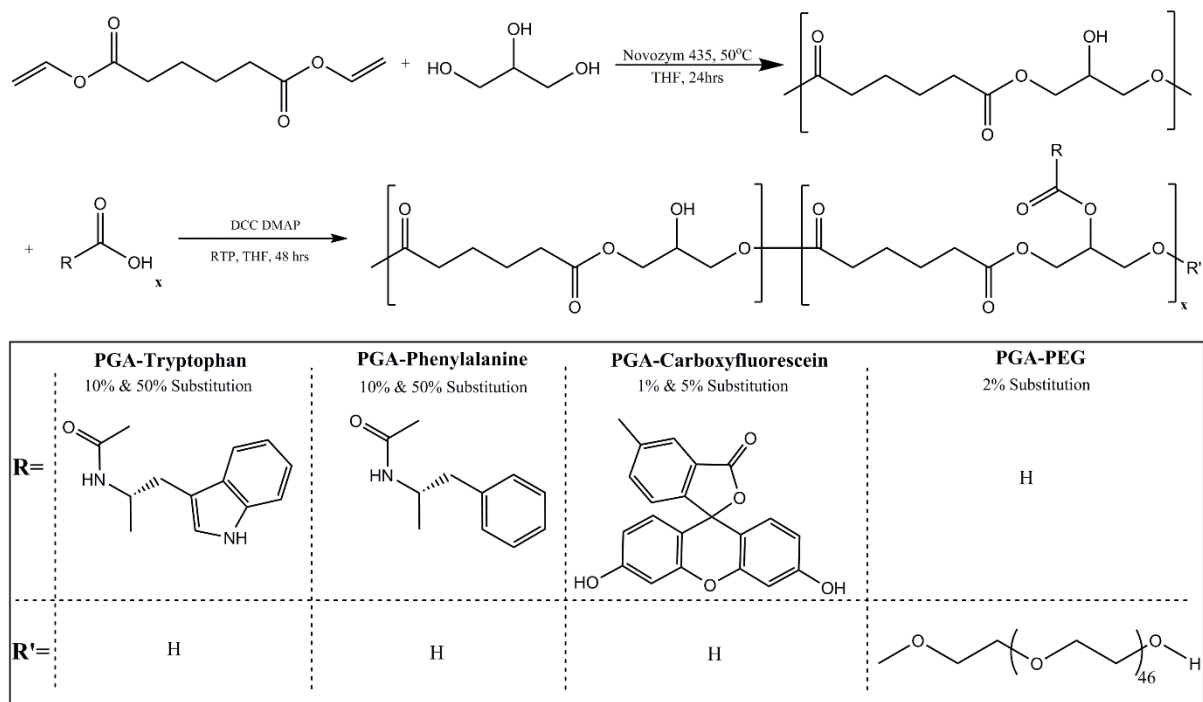
- 1181
1182
1183 applications, RSC Adv. 6 (2016) 109401–109405. doi:10.1039/c6ra21464a.
1184
1185 [9] V. Taresco, J. Suksiriworapong, R. Creasey, J.C. Burley, G. Mantovani, C. Alexander,
1186 K. Treacher, J. Booth, M.C. Garnett, Properties of acyl modified poly(glycerol-
1187 adipate) comb-like polymers and their self-assembly into nanoparticles, J. Polym. Sci.
1188 Part A Polym. Chem. 54 (2016) 3267–3278. doi:10.1002/pola.28215.
1189
1190 [10] S. Puri, P. Kallinteri, S. Higgins, G.A. Hutcheon, M.C. Garnett, Drug incorporation
1191 and release of water soluble drugs from novel functionalised poly(glycerol adipate)
1192 nanoparticles, J. Control. Release. 125 (2008) 59–67.
1193 doi:10.1016/j.jconrel.2007.09.009.
1194
1195 [11] T. Wersig, M.C. Hacker, J. Kressler, K. Mäder, Poly(glycerol adipate) – indomethacin
1196 drug conjugates – synthesis and in vitro characterization, Int. J. Pharm. 531 (2017)
1197 225–234. doi:10.1016/J.IJPHARM.2017.08.093.
1198
1199 [12] J. Suksiriworapong, V. Taresco, D.P. Ivanov, I.D. Styliari, K. Sakchaisri, V.B.
1200 Junyaprasert, M.C. Garnett, Synthesis and properties of a biodegradable polymer-drug
1201 conjugate: Methotrexate-poly(glycerol adipate), Colloids Surfaces B Biointerfaces.
1202 167 (2018) 115–125. doi:10.1016/j.colsurfb.2018.03.048.
1203
1204 [13] C.J. Thompson, D. Hansford, D.L. Munday, S. Higgins, C. Rostron, G.A. Hutcheon,
1205 Synthesis and Evaluation of Novel Polyester-Ibuprofen Conjugates for Modified Drug
1206 Release, Drug Dev. Ind. Pharm. 34 (2008) 877–884.
1207 doi:10.1080/03639040801929075.
1208
1209 [14] M. Dunne, O.I. Corrigan, Z. Ramtoola, Influence of particle size and dissolution
1210 conditions on the degradation properties of polylactide-co-glycolide particles,
1211 Biomaterials. 21 (2000) 1659–1668. doi:10.1016/S0142-9612(00)00040-5.
1212
1213 [15] E. Marin, M.I. Briceño, C. Caballero-George, Critical evaluation of biodegradable
1214 polymers used in nanodrugs, Int. J. Nanomedicine. 8 (2013) 3071–3091.
1215 doi:10.2147/IJN.S47186.
1216
1217 [16] J. Park, M. Ye, K. Park, Biodegradable Polymers for Microencapsulation of Drugs,
1218 Molecules. 10 (2005) 146–161. doi:10.3390/10010146.
1219
1220 [17] T. Tarvainen, M. Malin, T. Suutari, M. Pöllänen, J. Tuominen, J. Seppälä, K. Järvinen,
1221 Pancreatin enhanced erosion of and macromolecule release from 2,2-bis(2-oxazoline)-
1222 linked poly(ϵ -caprolactone), J. Control. Release. 86 (2003) 213–222.
1223 doi:10.1016/S0168-3659(02)00372-3.
1224
1225 [18] M. Longmire, P.L. Choyke, H. Kobayashi, Clearance properties of nano-sized particles
1226 and molecules as imaging agents: considerations and caveats., Nanomedicine. 3 (2008)
1227 703–17. doi:10.2217/17435889.3.5.703.
1228
1229 [19] H.S. Azevedo, R.L. Reis, Understanding the Enzymatic Degradation of Biodegradable
1230 Polymers and Strategies to Control Their Degradation Rate, in: Biodegrad. Syst.
1231 Tissue Eng. Regen. Med., CRC Press, Boca Raton, FL, 2005: pp. 177–201.
1232
1233 [20] Q. Chen, X. Yang, Y. Li, A comparative study on in vitro enzymatic degradation of
1234
1235
1236
1237
1238
1239

- 1240
1241
1242 poly(glycerol sebacate) and poly(xylitol sebacate), *RSC Adv.* 2 (2012) 4125–4134.
1243 doi:10.1039/c2ra20113e.
1244
- 1245 [21] I. Pomerantseva, N. Krebs, A. Hart, C.M. Neville, A.Y. Huang, C.A. Sundback,
1246 Degradation behavior of poly(glycerol sebacate), *J. Biomed. Mater. Res. Part A.* 4
1247 (2008) 1038–47. doi:10.1002/jbm.a.32327.
1248
- 1249 [22] S. Liang, X. Yang, X. Fang, W.D. Cook, G.A. Thouas, Q. Chen, In Vitro enzymatic
1250 degradation of poly(glycerol sebacate) -based materials, *Biomaterials.* 32 (2011)
1251 8486–8496. doi:10.1016/j.biomaterials.2011.07.080.
1252
- 1253 [23] M.M. Muley, A.R. Reid, B. Botz, K. Bölskei, Z. Helyes, J.J. McDougall, Neutrophil
1254 elastase induces inflammation and pain in mouse knee joints via activation of
1255 proteinase-activated receptor-2., *Br. J. Pharmacol.* 173 (2016) 766–77.
1256 doi:10.1111/bph.13237.
1257
- 1258 [24] Sigma-Aldrich, Elastase (EC 3.4.21.36) continuous spectrophotometric rate assay,
1259 (n.d.). [http://www.sigmaaldrich.com/technical-](http://www.sigmaaldrich.com/technical-documents/protocols/biology/enzymatic-assay-of-elastase.html)
1260 [documents/protocols/biology/enzymatic-assay-of-elastase.html](http://www.sigmaaldrich.com/technical-documents/protocols/biology/enzymatic-assay-of-elastase.html) (accessed March 7,
1261 2017).
1262
- 1263 [25] Sigma-Aldrich, Enzymatic Assay of Esterase, (n.d.).
1264 [http://www.sigmaaldrich.com/technical-documents/protocols/biology/enzymatic-](http://www.sigmaaldrich.com/technical-documents/protocols/biology/enzymatic-assay-of-esterase.html)
1265 [assay-of-esterase.html](http://www.sigmaaldrich.com/technical-documents/protocols/biology/enzymatic-assay-of-esterase.html) (accessed March 7, 2017).
1266
- 1267 [26] Sigma-Aldrich, Procedure for Enzymatic Assay of Trypsin (EC 3.4.21.4), (n.d.).
1268 [http://www.sigmaaldrich.com/technical-documents/protocols/biology/enzymatic-](http://www.sigmaaldrich.com/technical-documents/protocols/biology/enzymatic-assay-of-trypsin.html)
1269 [assay-of-trypsin.html](http://www.sigmaaldrich.com/technical-documents/protocols/biology/enzymatic-assay-of-trypsin.html) (accessed March 7, 2017).
1270
- 1271 [27] C. Colombo, L. Dragoni, S. Gatti, R.M. Pesce, T.R. Rooney, E. Mavroudakakis, D.
1272 Moscatelli, Tunable Degradation Behavior of PEGylated Polyester-Based
1273 Nanoparticles Obtained Through Emulsion Free Radical Polymerization., *Ind. Eng.*
1274 *Chem. Reseach.* 53 (2014) 9128–9135. doi:10.1021/ie4036077.
1275
- 1276 [28] O. Warburg, The Metabolism of Carcinoma Cells, *J. Cancer Res.* 9 (1925) 148–163.
1277 doi:10.1158/jcr.1925.148.
1278
- 1279 [29] O. Warburg, F. Wind, N. Negelein, The Metabolism of Tumors in the Body, *J. Gen.*
1280 *Physiol.* 8 (1927) 519–530. doi:10.1085/jpg.8.6.519.
1281
- 1282 [30] N. Kamaly, B. Yameen, J. Wu, O.C. Farokhzad, Degradable Controlled-Release
1283 Polymers and Polymeric Nanoparticles: Mechanisms of Controlling Drug Release,
1284 *Chem. Rev.* 116 (2016) 2602–2663. doi:10.1021/acs.chemrev.5b00346.
1285
- 1286 [31] Malvern Panalytical, Zetasizer Nano ZS, (2018).
1287 [https://www.malvernpanalytical.com/en/products/product-range/zetasizer-](https://www.malvernpanalytical.com/en/products/product-range/zetasizer-range/zetasizer-nano-range/zetasizer-nano-zs)
1288 [range/zetasizer-nano-range/zetasizer-nano-zs](https://www.malvernpanalytical.com/en/products/product-range/zetasizer-range/zetasizer-nano-range/zetasizer-nano-zs) (accessed September 27, 2018).
1289
- 1290 [32] M. Labet, W. Thielemans, Synthesis of polycaprolactone: a review, *Chem. Soc. Rev.*
1291 38 (2009) 3484–3504. doi:10.1039/b820162p.
1292
1293
1294
1295
1296
1297
1298

- 1299
1300
1301
1302
1303
1304
1305
1306
1307
1308
1309
1310
1311
1312
1313
1314
1315
1316
1317
1318
1319
1320
1321
1322
1323
1324
1325
1326
1327
1328
1329
1330
1331
1332
1333
1334
1335
1336
1337
1338
1339
1340
1341
1342
1343
1344
1345
1346
1347
1348
1349
1350
1351
1352
1353
1354
1355
1356
1357
- [33] J.S. Suk, Q. Xu, N. Kim, J. Hanes, L.M. Ensign, PEGylation as a strategy for improving nanoparticle-based drug and gene delivery., *Adv. Drug Deliv. Rev.* 99 (2016) 28–51. doi:10.1016/j.addr.2015.09.012.
- [34] J. V Olsen, S.-E. Ong, M. Mann, Trypsin cleaves exclusively C-terminal to arginine and lysine residues, *Mol. Cell. Proteomics.* 3 (2004) 608–14. doi:10.1074/mcp.T400003-MCP200.
- [35] A.A. Mendes, P.C. Oliveira, H.F. De Castro, Properties and biotechnological applications of porcine pancreatic lipase, *J. Mol. Catal. B Enzym.* 78 (2012) 119–134. doi:10.1016/j.molcatb.2012.03.004.
- [36] M.M. Burrell, *Enzymes in Molecular Biology*, in: J.M. Walker (Ed.), *Methods Mol. Biol.*, Humana Press, Totawa, New Jersey, 1993: pp. 283–284.
- [37] W. Bode, E. Meyer, J.C. Powers, Human Leukocyte and Porcine Pancreatic Elastase: X-ray Crystal Structures, Mechanism, Substrate Specificity, and Mechanism-Based Inhibitors, *Biochemistry.* 28 (1989) 1951–1963. doi:10.1021/bi00431a001.
- [38] E.J. Toone, M.J. Werth, J.B. Jones, Active-Site Model for Interpreting and Predicting the Specificity of Pig Liver Esterase, *J. Am. Chem. Soc.* 112 (1990) 4946–4952. doi:10.1021/ja00168a047.

1417
1418
1419
1420 **Figures**

1421 **Figure 1**



1444
1445 *Fig. 1: Synthesis and Modification of PGA.* The reaction scheme for the synthesis of PGA
1446 and subsequent modification by Steglich Esterification is shown here. Adapted from Taresco
1447 et al.[1,4]

Figure 2

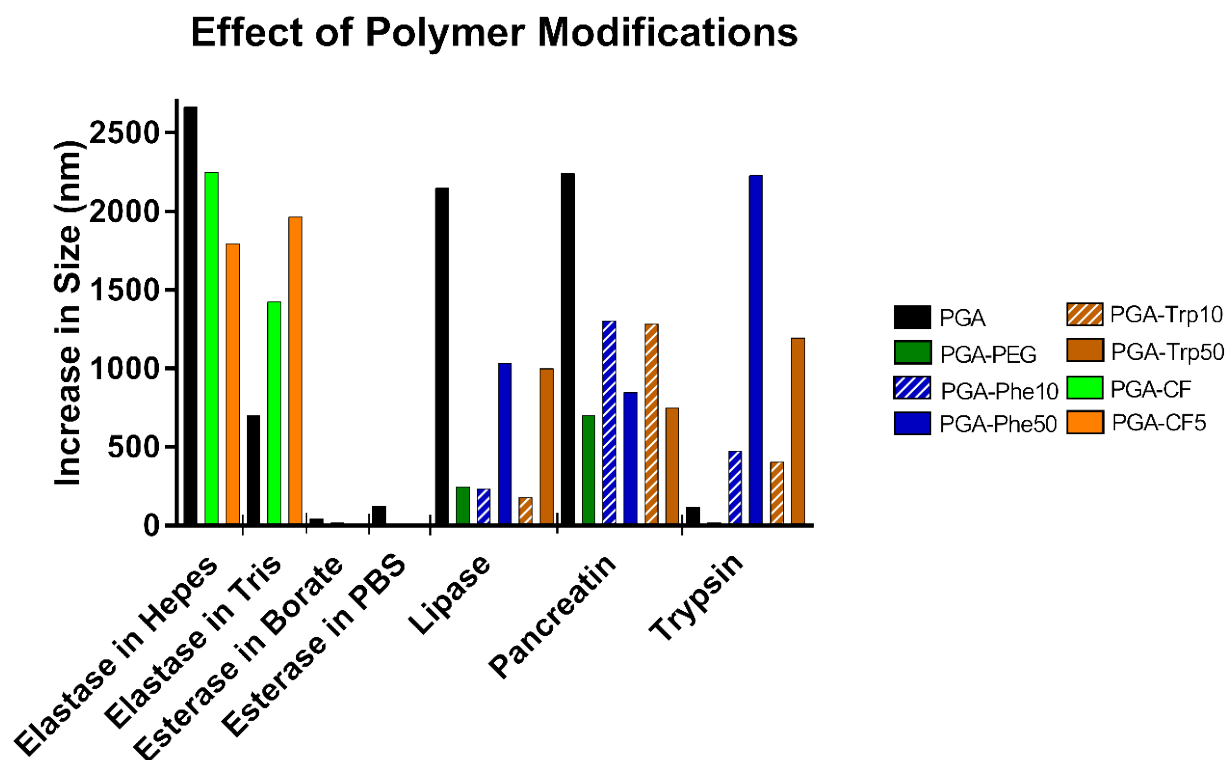


Fig. 2: Effect of Backbone Modifications on PGA Degradation. The colour of each bar here reflects the polymer under investigation. The results for pepsin have been omitted as it was not possible to differentiate the effect of the enzyme from that of the buffer.

Figure 3 A-C

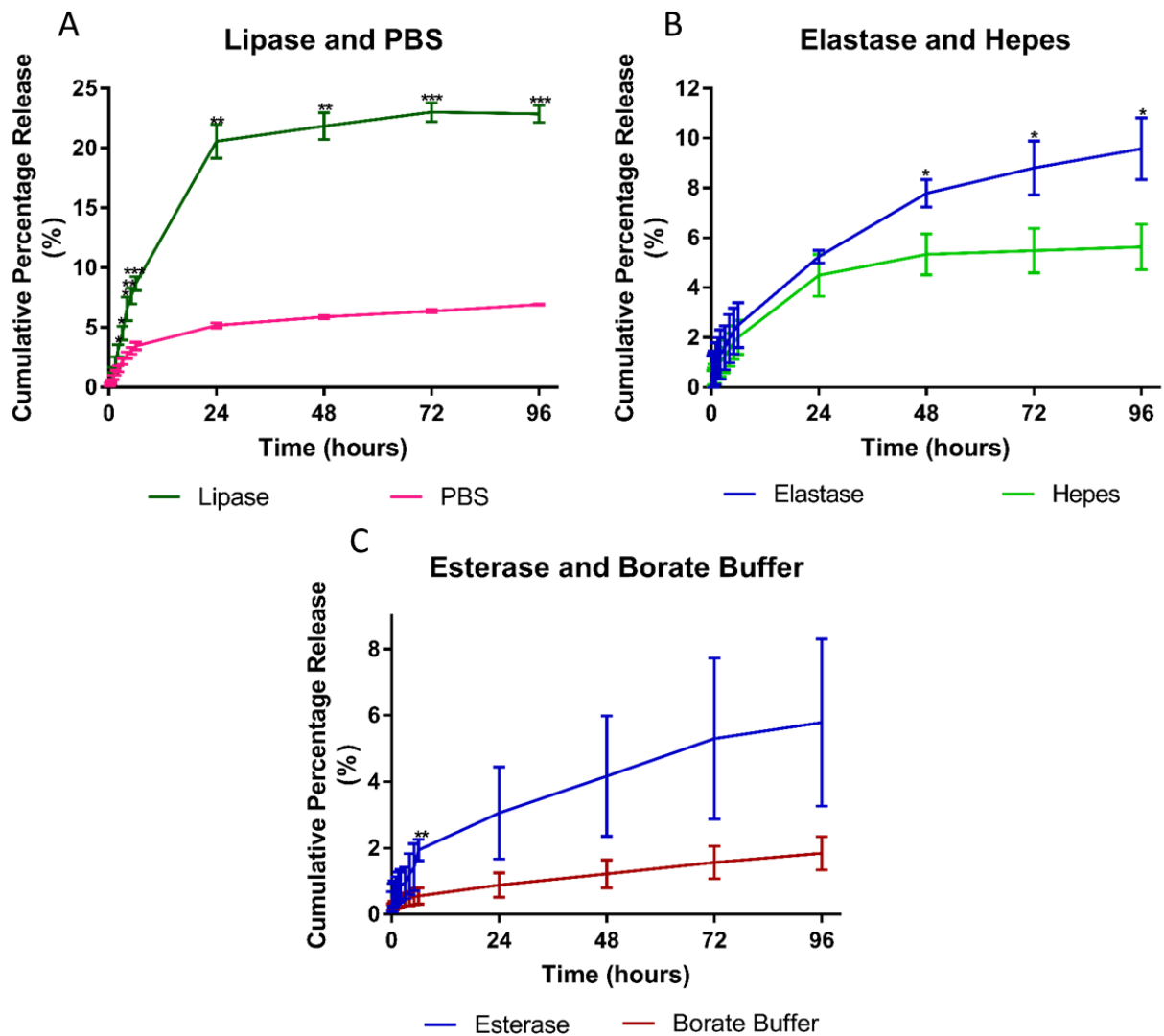


Fig.3 A-C: Release of Carboxyfluorescein in the Presence of Lipase, Elastase and Esterase. The release of carboxyfluorescein in the presence of lipase, elastase and esterase is shown in A, B & C, respectively and each graph also shows the relevant buffer control. The points used here are the average of three experiments whereas the error bars represent 1 standard deviation. Calculated p-values for each time point, comparing release with and without the enzyme are indicated by asterisks.

Figure 4 A & B:

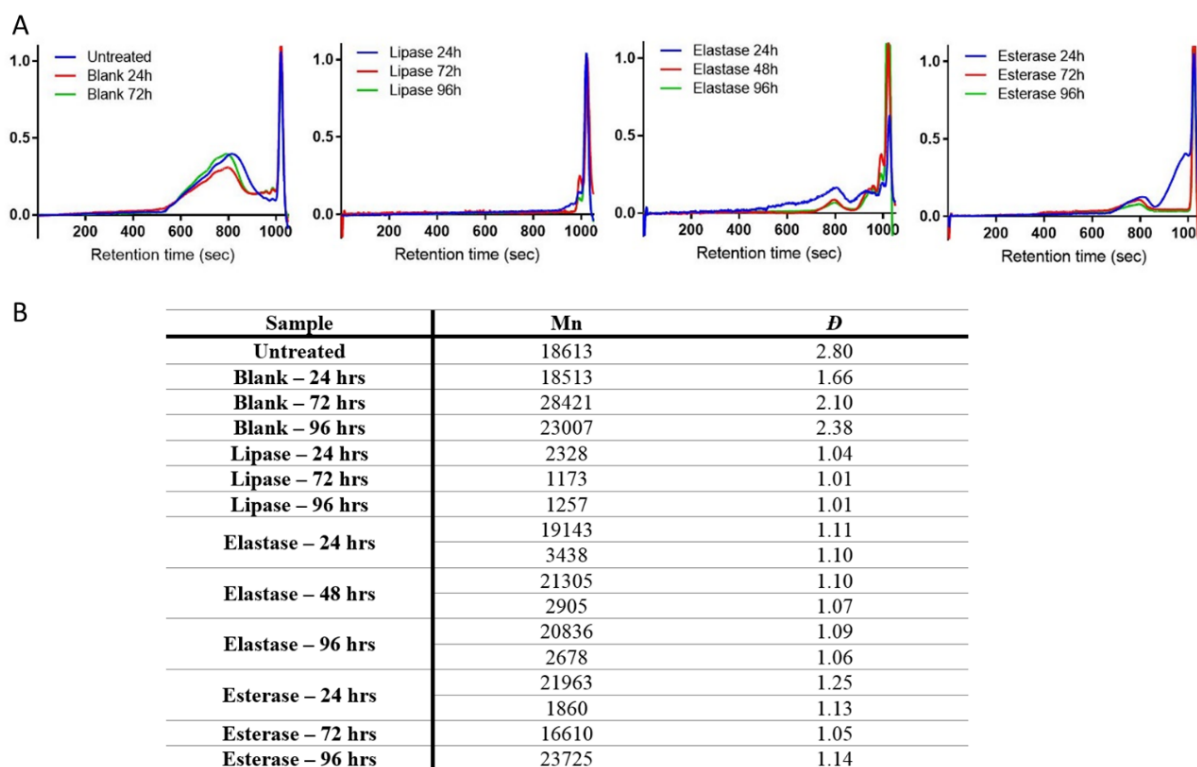
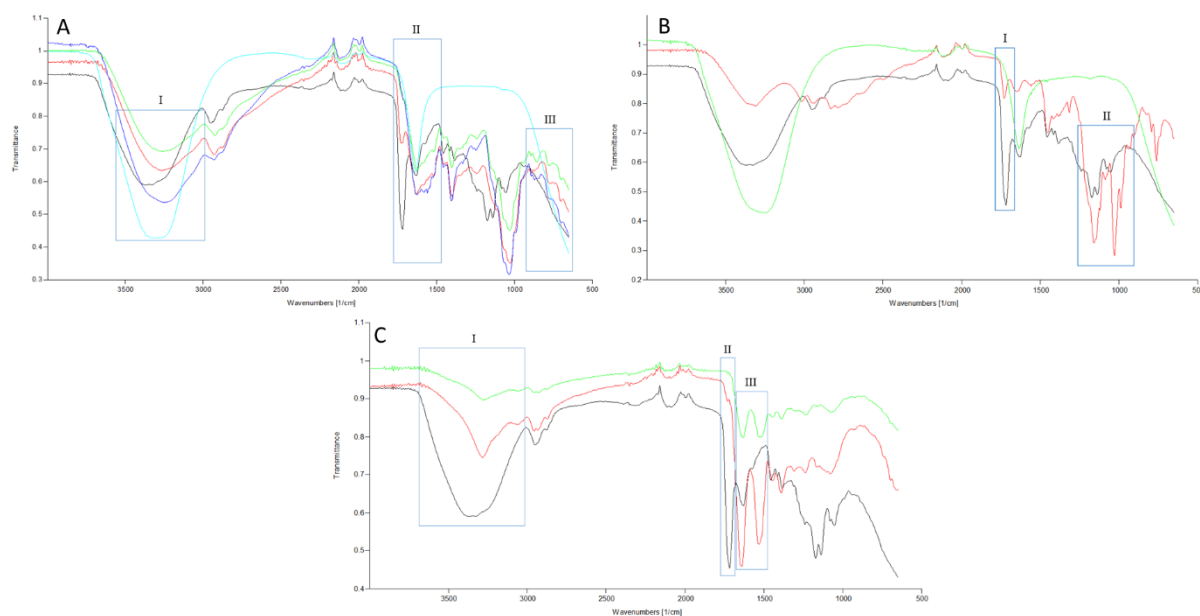


Fig. 4 A & B: GPC Traces, Molecular Weight and Polydispersity of PGA-CF5 Following Enzyme Incubation. In A the traces for each sample are presented, grouped by enzyme. The large peaks seen in the region of 1000 seconds represent the eluent. There is little difference between the untreated sample and the blank samples, incubated without enzyme, suggesting the changes seen upon incubation with enzymes are as a result of enzymatic degradation. In B the number average molecular weight (Mn) and Polydispersity (\bar{D}) are listed.

1653
1654
1655 **Figure 5 A-C**
1656
1657



1667
1668
1669
1670
1671
1672
1673
1674
1675
1676
1677 *Fig. 5 A-C: FTIR Spectra of PGA-CF5 Before and After Incubation with Enzymes.* Incubation
1678 with lipase is shown in A, elastase in B and esterase in C. The key differences in the spectra
1679 are highlighted with blue boxes and the peak allocation is discussed in the text. In all cases
1680 the spectrum for untreated PGA-CF5 is shown in black. For lipase (A) PGA-CF5 after 24
1681 hours incubation with lipase is in red; 72 hours incubation is in green and 96 hours incubation
1682 is in dark blue. Lipase alone is shown in sky blue. For elastase and esterase (B & C), PGA-
1683 CF5 incubated with the respective enzyme is shown in red and the enzyme alone is shown in
1684 green.
1685
1686
1687
1688
1689
1690
1691
1692
1693
1694
1695
1696
1697
1698
1699
1700
1701
1702
1703
1704
1705
1706
1707
1708
1709
1710
1711

Figure 6 A-D

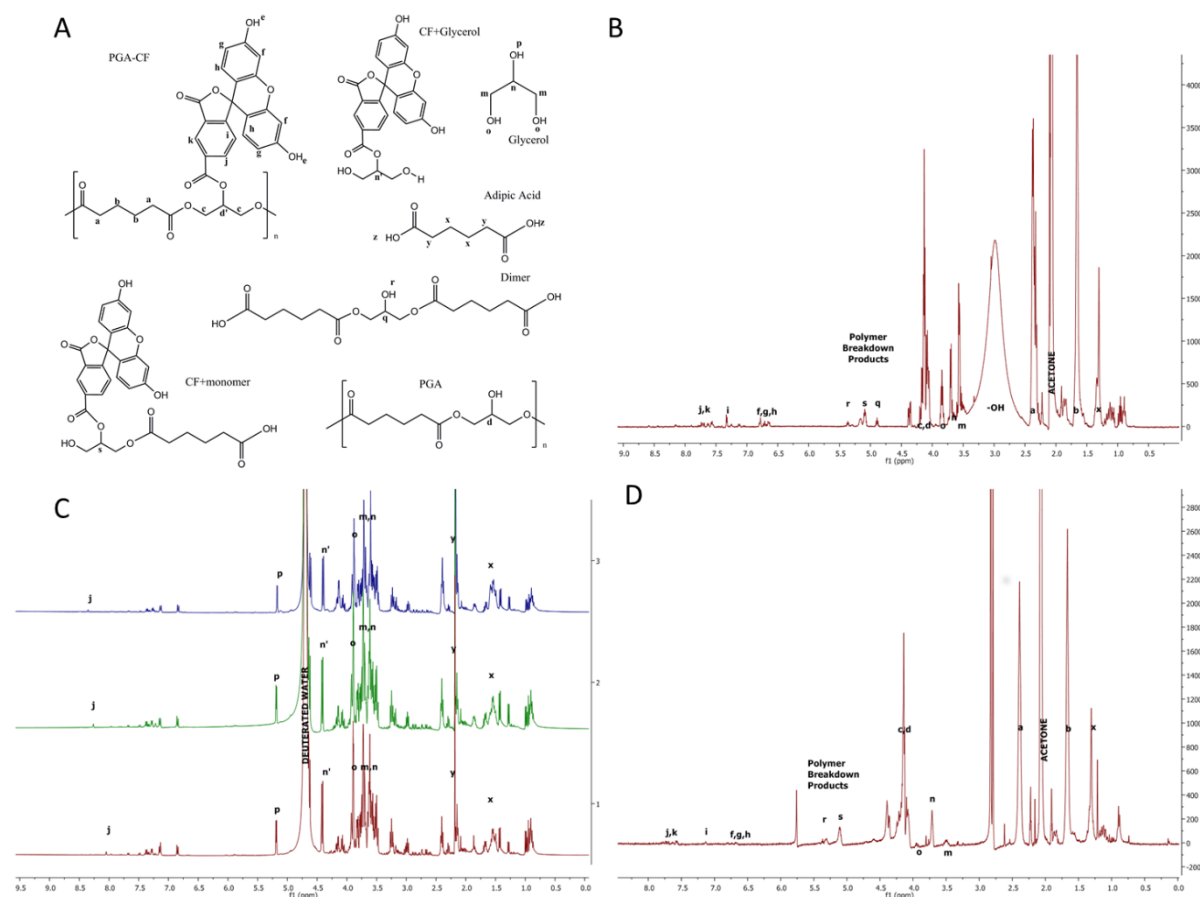


Fig. 6 A-D: NMR Spectra of PGA-CF5 Incubated with Enzymes and Corresponding Labeled Structures: The labelled structures shown in A correspond with each of the following spectra examining degradation by lipase, elastase and esterase in acetone-d6 and deuterium oxide. The spectrum in B is PGA-CF5 after incubation for 24 hours in lipase, analysed in acetone-d6. The spectra for 72 & 96 hours were very similar, and so are not shown here. In C analysis was carried out in deuterium oxide. The top spectrum is after 24 hours of incubation with lipase, the middle spectrum after 72 hours and the bottom spectrum after 96 hours. The spectrum in D is PGA-CF5 following incubation with esterase, analysed in acetone-d6. The key difference between this spectrum and those for elastase and lipase is the absence of one peak from the area labelled 'Polymer Breakdown Products'.

Supplementary Information

Appendix A

¹H NMR was used to confirm the success of the polymer couplings and to provide an estimate of the substitution ratio. The coupled polymer was dissolved in acetone-d₆ and analysed by ¹H NMR.

A.1 PGA-Carboxyfluorescein – Low Substitution

The presence of peaks at 6.5-7.0 ppm, 8.15 ppm and 9.75 ppm confirm the presence of carboxyfluorescein in the polymer and consequently the success of the coupling [Fig. A.1]. The aim was to achieve one dye molecule coupled to each polymer chain and 17% conversion was achieved, meaning a dye molecule was coupled to 17% of polymer chains.

Fig A.1: NMR Spectrum of PGA-Carboxyfluorescein at Low Substitution. The peaks relating to carboxyfluorescein can be seen on the left-hand side of the spectrum whereas those from PGA are on the right-hand side. The integrals of the peaks labelled 'b', from the PGA, and 'f, g, h', from the carboxyfluorescein were used to calculate the substitution ratio.

A.2 PGA-Carboxyfluorescein 5%

The presence of the peaks representing carboxyfluorescein again confirm that the coupling was successful [Fig. A.2]. In this case the substitution ratio was found to be 1.7%, representing a conversion of 34%. PGA-CF5 was continued to be used to refer to this polymer as it represents the targeted substitution level.

Fig. A.2: NMR Spectrum of PGA-CF5. As with PGA-CF [Fig A.1] the integrals of the peaks labelled 'f, g, h' (carboxyfluorescein) were used to calculate the amount of carboxyfluorescein, relative to peak b (PGA). The substitution was estimated to be 1.7%.

A.3 PGA-PEG

The peak representing the protons of the repeating unit of PEG, labelled 'e', was used to confirm the coupling was successful and to provide an estimate of the substitution ratio; this was calculated to be 1 unit of PEG per PGA polymer chain, as was the target of the substitution [Fig. A.3].

1830
1831
1832
1833
1834
1835
1836
1837
1838
1839
1840
1841
1842
1843
1844
1845
1846
1847
1848
1849
1850
1851
1852
1853
1854
1855
1856
1857
1858
1859
1860
1861
1862
1863
1864
1865
1866
1867
1868
1869
1870
1871
1872
1873
1874
1875
1876
1877
1878
1879
1880
1881
1882
1883
1884
1885
1886
1887
1888

Fig. A.3: NMR Spectrum of PGA-PEG. The peak labelled 'e' represents the protons of PEG adjacent to the ester bond, and was consequently used to confirm the successful coupling and to predict the substitution ratio.

Appendix B

B.1 Elastase

The method for this assay was taken from the technical documents and protocols section of the Sigma-Aldrich website.[1] One unit of elastase is defined as the amount that will hydrolyse 1.0 μ mole of N-succinyl-L-Ala-Ala-Ala-p-nitroanilide per minute at pH 8.0 at 25 °C in Tris buffer (0.1 mM). This was measured by following the increase in absorbance at 410 nm over 6 minutes by UV Spectrophotometry (Beckman Coulter DU800, High Wycombe). Two blanks, with the substrate but no enzyme, and six enzyme samples were analysed.

This activity assay was carried out before each experiment involving elastase; an example of the results obtained is presented here. The activity appeared to be fairly consistent between samples [Fig B.1]. The average activity of the original preparation was calculated to be 8.97 units/ml (SD=2.36).

Fig. B.1: Elastase Activity Assay. The change in absorbance at 410 nm is plotted against the time in minutes. Although measurements were taken throughout the 6 minutes only the linear portions are shown here, as recommended in the method. The line of best fit was used to calculate the change in absorbance, and consequently the activity, for each sample. These lines all had a R^2 value >0.985 .

B.2 Esterase

This method was taken from Sigma-Aldrich[2], whereby one unit is defined as the amount that will hydrolyse 1.0 μ mole of ethyl butyrate to butyric acid and ethanol per minute at pH 8.0 at 25 °C in borate buffer (10 mM). This is a titrimetric assay, based around the time taken for the pH to return to 8.0 following the addition of NaOH (0.01 N) (Jenway 3505 pH meter, Stone, Staffordshire). One blank, with the substrate but no enzyme, and three enzyme-containing samples were analysed.

Again, one example of the activity assay, which was performed multiple times, is presented here. As with elastase, the activity appeared to be relatively constant between samples [Fig. B.2]. The average activity of the original preparation was calculated to be 15.06 units/mg (SD=1.25).

1948
1949
1950
1951
1952
1953
1954
1955
1956
1957
1958
1959
1960
1961
1962
1963
1964
1965
1966
1967
1968
1969
1970
1971
1972
1973
1974
1975
1976
1977
1978
1979
1980
1981
1982
1983
1984
1985
1986
1987
1988
1989
1990
1991
1992
1993
1994
1995
1996
1997
1998
1999
2000
2001
2002
2003
2004
2005
2006

Fig. B.2: Esterase Activity Assay. This graph charts the additions of NaOH made and the time points at which this occurred. As with the elastase activity assay, only the linear portions are shown here to aid clarity. The lines of best fit all had R^2 values >0.99 . The blank is not shown as the pH did not return to 8.0 for the duration of the assay. The gradient of the line was taken as the rate of change and then corrected for the blank; this figure was used to calculate the activity.

B.3 Lipase

A suitable, pre-determined, method could not be found for the lipase activity assay. The reagents required for those that were available and commercially available kits were considered to be prohibitively expensive for the intended use. Therefore, a novel method was devised based on several pre-existing literature methods.[3–5]

4-methylumbellifyl butyrate (4-MUB) was used as the substrate; lipase cleaves the butyrate group to produce 4-methyl umbelliferone (4-MU) which is fluorescently active. 4-MUB (6.2 mg) was dissolved in DMSO (1.5 ml) before diluting to a concentration of 1 mM with ultrapure water (25 ml). It has been noted that 4-MUB will slowly crystallise out of this solution,[5] and so this was prepared immediately prior to use and shaken vigorously before each 300 μ l aliquot was added to the reaction. The reaction was performed in Tris buffer (pH 7.5, 0.2 M) with a total reaction volume of 3 ml per assay. Enzyme solution (50 μ l, 1 mg/ml in buffer) was added immediately before commencing measurement of the fluorescence intensity (Excitation 365 nm, Emission 445 nm). The intensity was measured every 15 seconds for at least 5 minutes using a Cary Eclipse Fluorescence Spectrophotometer (Agilent Technologies, Santa Clara, CA). Five enzyme samples were tested along with two blank samples containing the substrate but no enzyme.

R^2 values of >0.98 were achieved for each of the five enzyme assays, suggesting good linearity [Fig. B.3]. The average change in intensity per minute was calculated to be 113.64 AU/min.

Fig B.3: Lipase Activity Assay. In this graph the linear portions are highlighted by black borders around the markers; these points were used to calculate the lines of best fit. At least five linear points were used for each sample. Whilst there is quite a difference in the intensities measured this was mainly a result of the time taken to begin the assay; the gradients of the lines for the enzyme samples are relatively similar.

2007
2008
2009
2010
2011
2012
2013
2014
2015
2016
2017
2018
2019
2020
2021
2022
2023
2024
2025
2026
2027
2028
2029
2030
2031
2032
2033
2034
2035
2036
2037
2038
2039
2040
2041
2042
2043
2044
2045
2046
2047
2048
2049
2050
2051
2052
2053
2054
2055
2056
2057
2058
2059
2060
2061
2062
2063
2064
2065

In order to quantify the results obtained a calibration of 4-MU fluorescence was performed. 4-MU (23.5 mg) was initially dissolved in DMSO (5 ml), and then 6 dilutions in ultrapure water were prepared and analysed [Fig. B.4]. The equation of the line of best fit was used to calculate the equivalent concentration of the change in intensity measured in the activity assay, giving a value of 21.54 nM/min. One unit was subsequently defined as the amount required to cleave 1.0 nmole of 4-MUB per minute in Tris buffer (pH 7.5, 0.2 M) at room temperature and with a total reaction volume of 3 ml.

Fig. B.4: Calibration of 4-Methyl Umbelliferone Fluorescence. The graph shows the calibration curve obtained for the fluorescence of 4-MU. The samples tested cover the full range of detectable intensities and a good R^2 value was obtained. Three readings were taken for each concentration; mean values are displayed on this graph. The equation of the line is displayed on the graph.

B.4 Trypsin

The method for this assay was taken from Sigma-Aldrich.[6] One unit was defined as the amount required to produce a change in absorbance at 253 nm of 0.001 per minute with Na-Benzoyl-L-arginine ethyl ester as the substrate with sodium phosphate monobasic buffer (67 mM, pH 7.6) at 25 °C in a reaction volume of 3.20 ml. The absorbance was measured by UV Spectrophotometry. Three enzyme samples were tested along with a blank with no enzyme.

The three results for enzyme activity were found to be particularly close, with the average activity calculated as 1558.2 units/mg with a standard deviation of 22.66 [Fig. B.5].

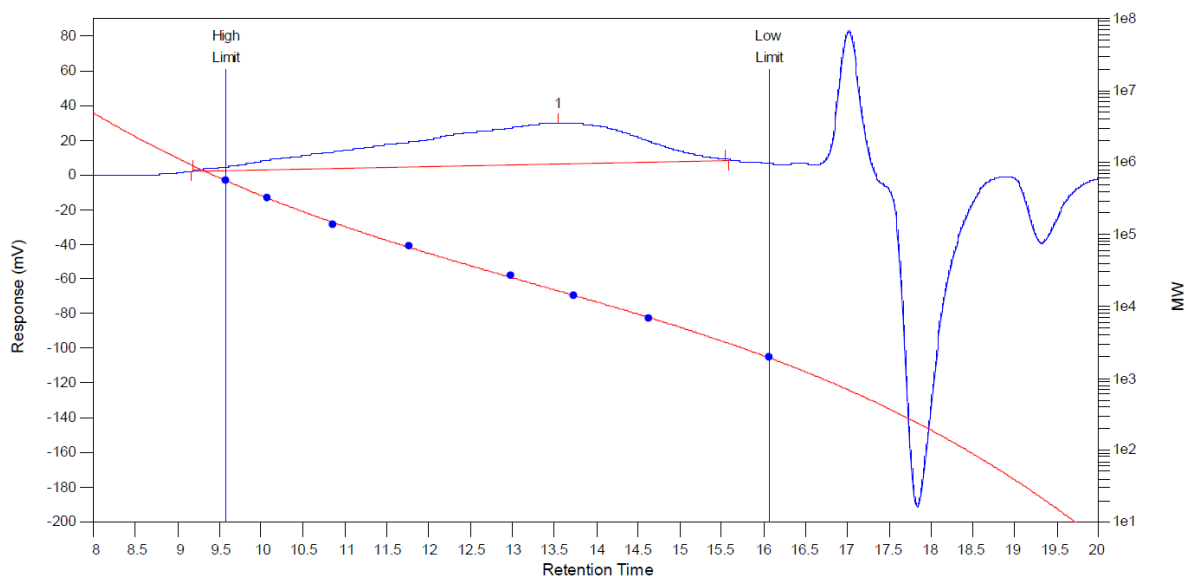
Fig. B.5: Trypsin Activity Assay. The absorbance at 253 nm is plotted against the time in minutes. As with the previous figures, only the linear portion is shown here. The absorbance values for the enzyme samples quickly exceeded 1, however, as the trend showed good linearity and all the lines of best fit had R^2 values >0.99 it was decided it would not be necessary to repeat the measurements.

Appendix C

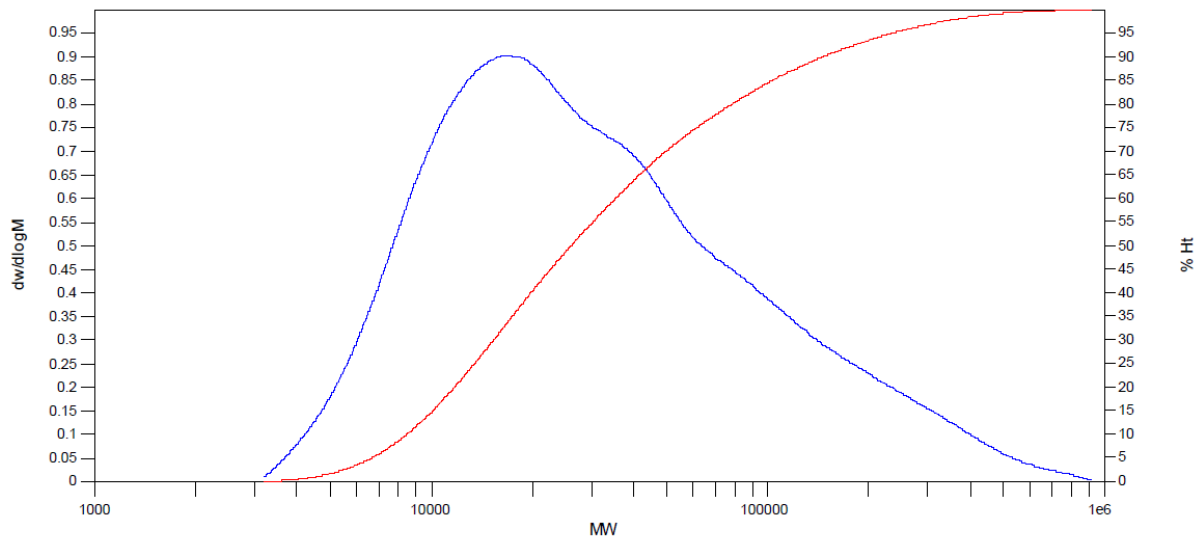
The GPC chromatograms and distribution plots for untreated PGA-CF5, polymer incubated without enzyme and polymer incubated with lipase, elastase or esterase follow. These results are discussed in detail in Section 3.3, p.15.

Untreated PGA-CF5

Chromatogram



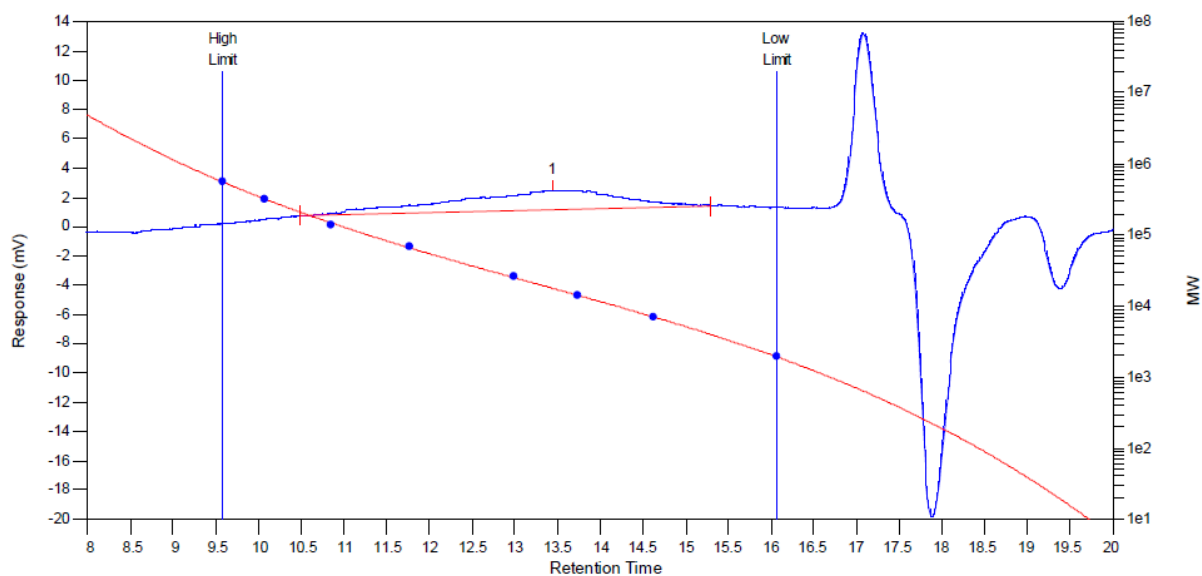
Distribution Plots



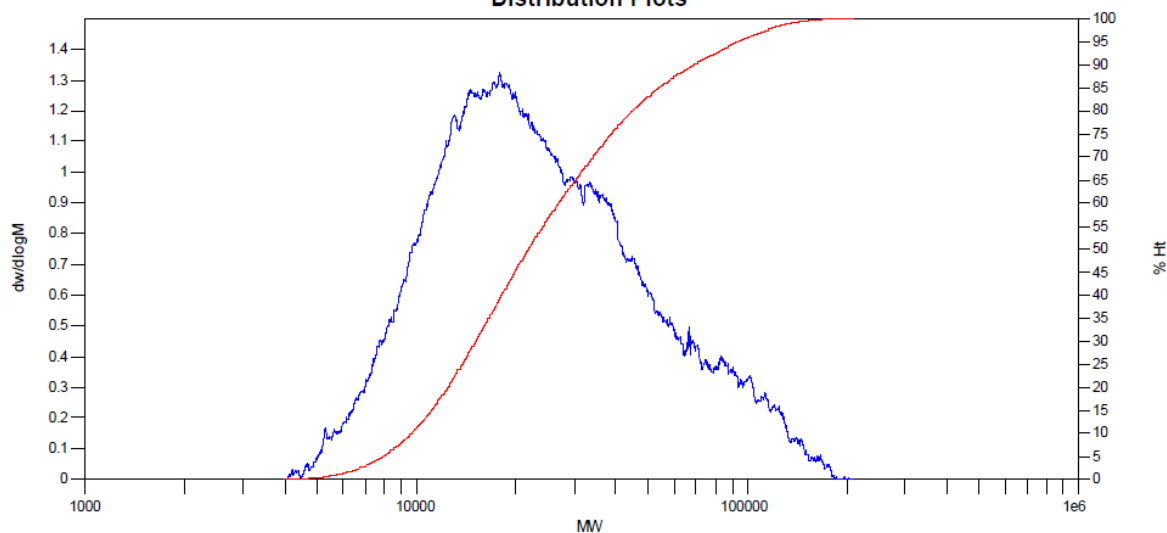
Peak No	Mp	Mn	Mw	Mz	Mz+1	Mv	PD
1	16482	18613	52062	168679	335720	42979	2.79708

Blank 24 hours

Chromatogram



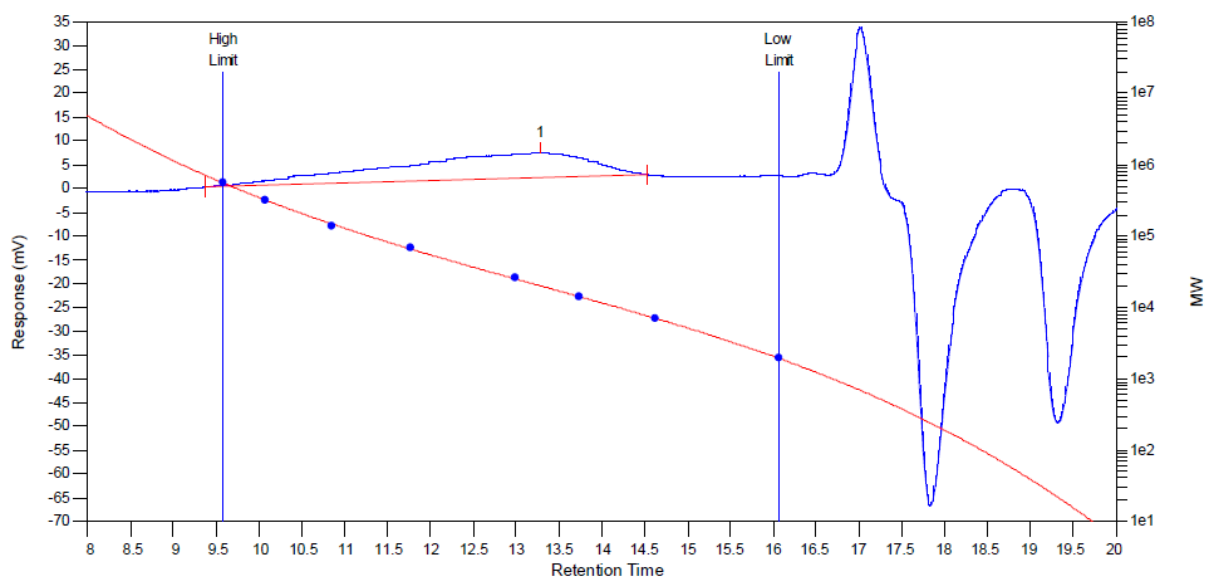
Distribution Plots



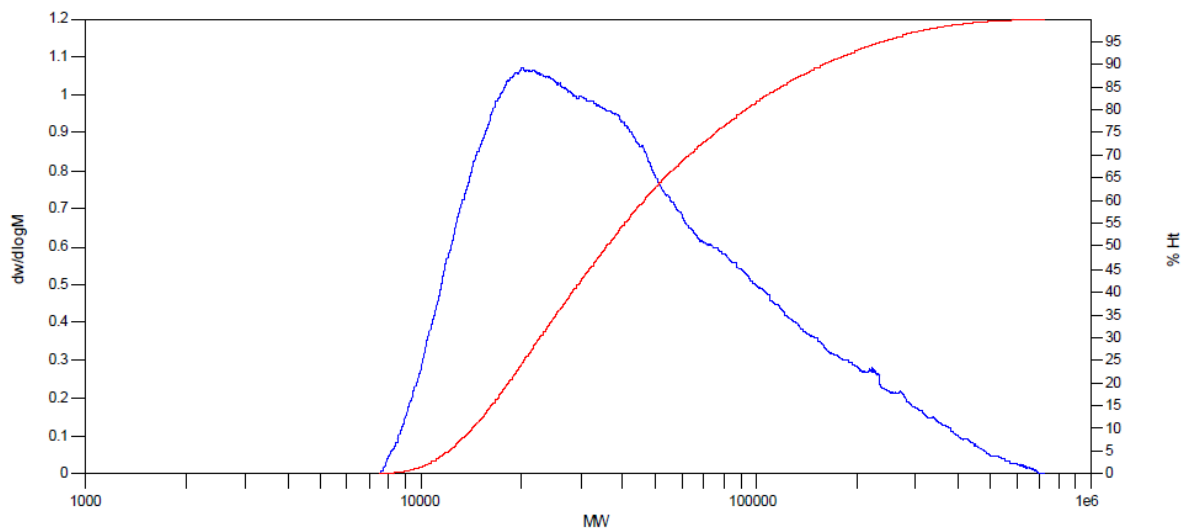
Peak No	Mp	Mn	Mw	Mz	Mz+1	Mv	PD
1	17860	18513	30797	53464	80776	28273	1.66353

Blank 72 hours

Chromatogram



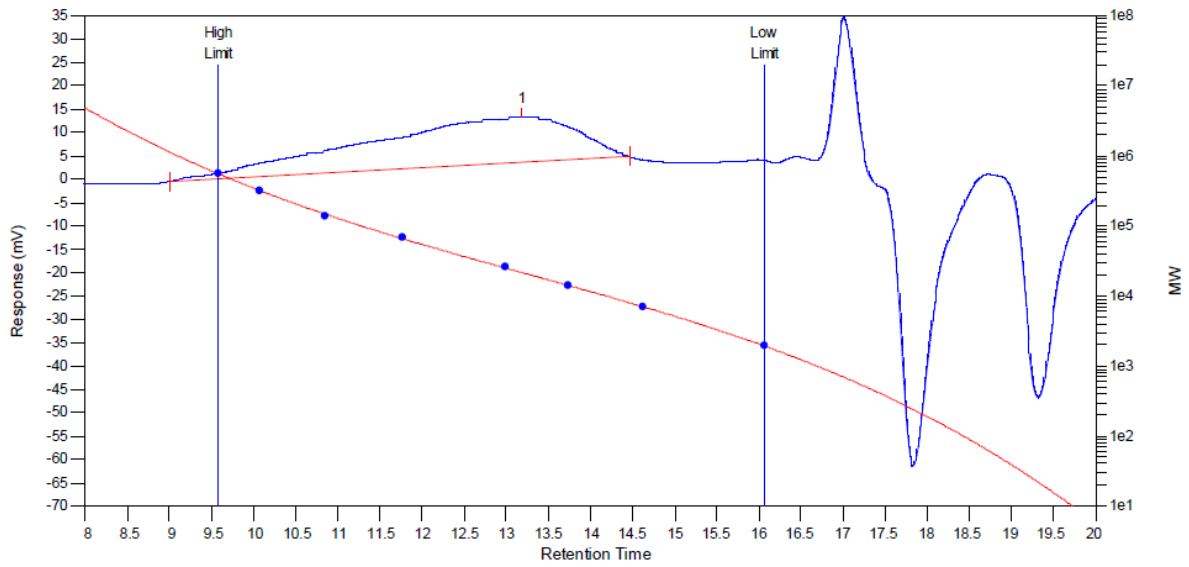
Distribution Plots



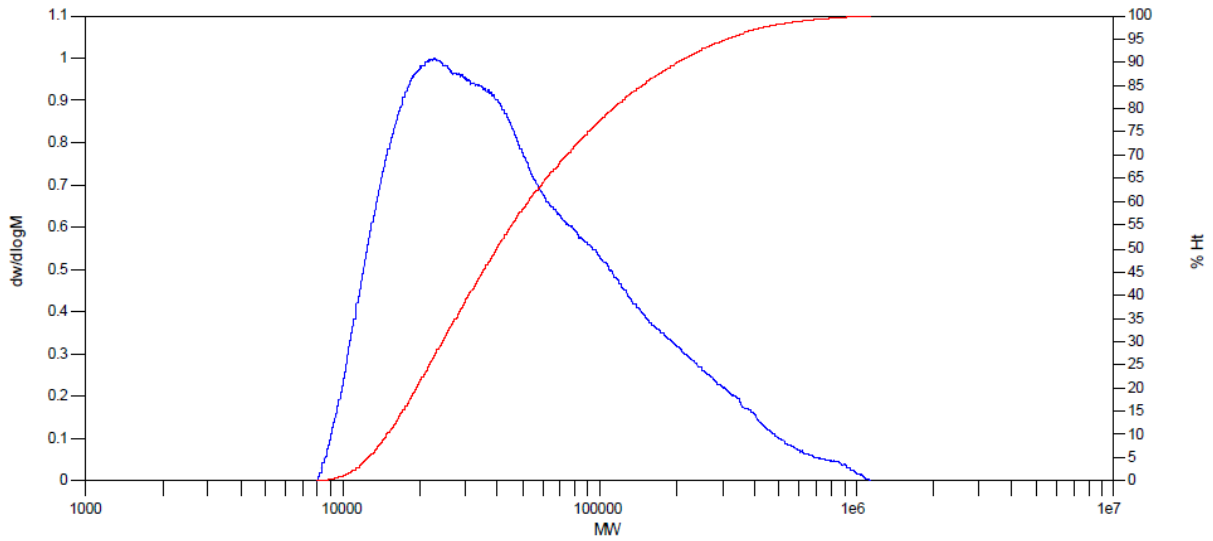
Peak No	Mp	Mn	Mw	Mz	Mz+1	Mv	PD
1	20181	28421	59816	147979	269242	51963	2.10464

Blank 96 hours

Chromatogram



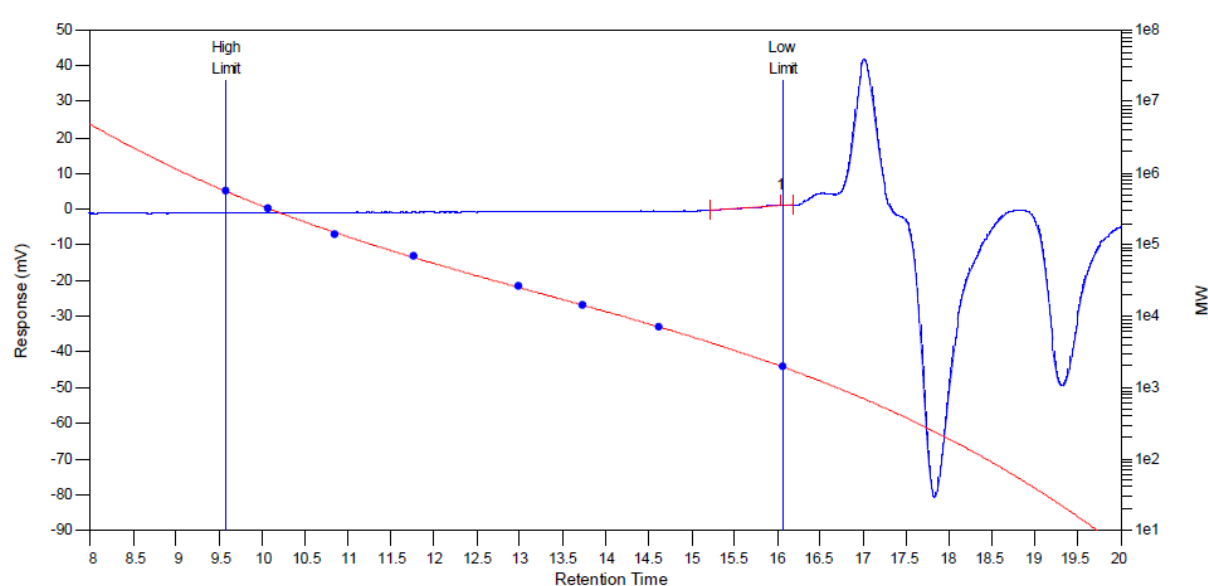
Distribution Plots



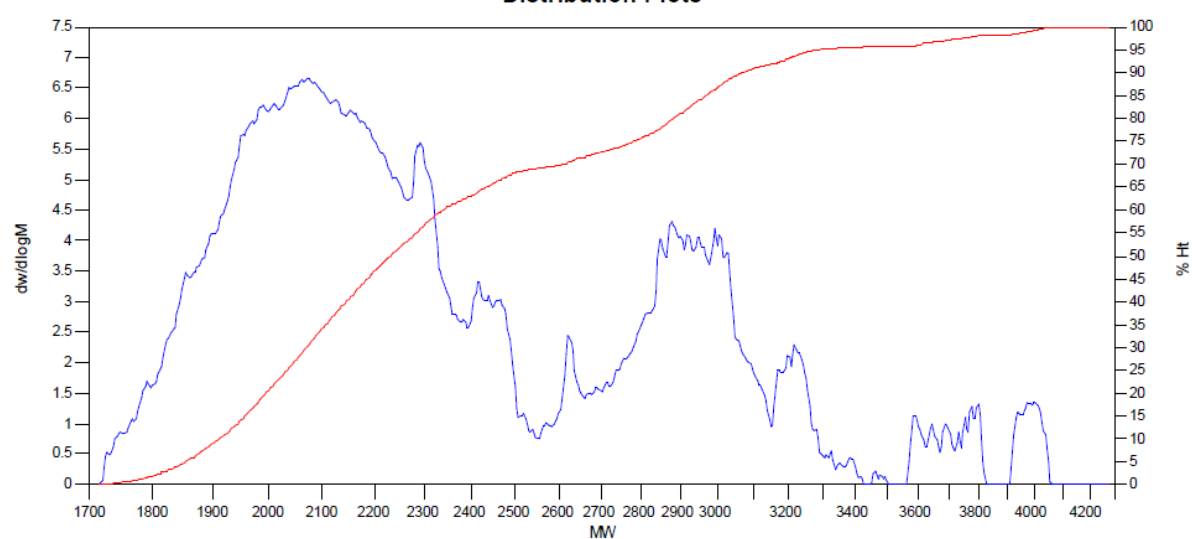
Peak No	Mp	Mn	Mw	Mz	Mz+1	Mv	PD
1	23007	30498	72569	216838	434991	61215	2.37947

Lipase 24 hours

Chromatogram



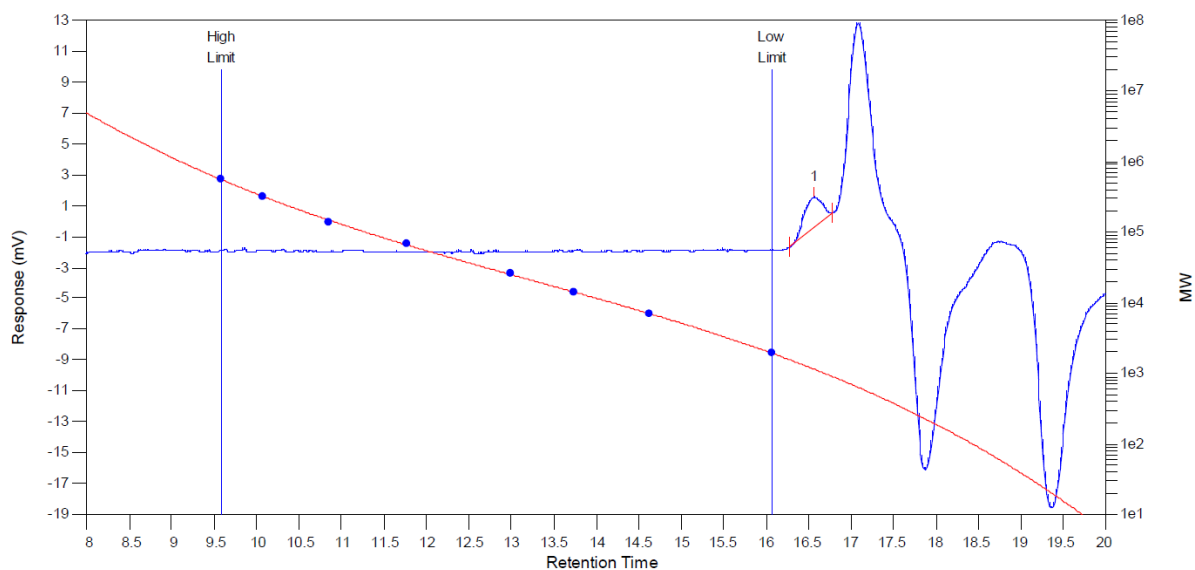
Distribution Plots



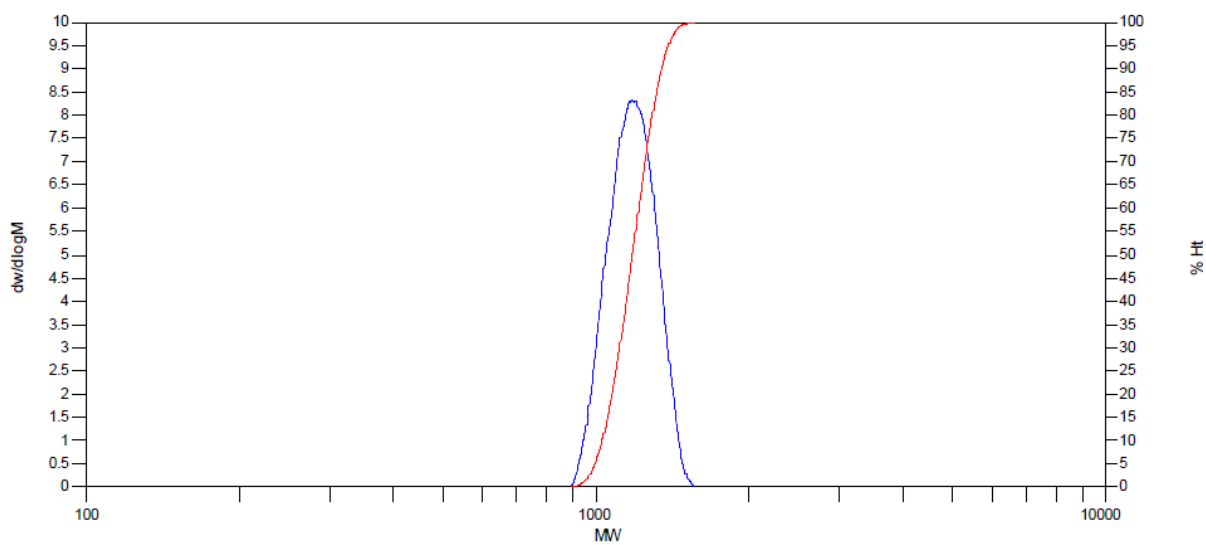
Peak No	Mp	Mn	Mw	Mz	Mz+1	Mv	PD
1	2073	2328	2418	2523	2643	2403	1.03866

Lipase 72 hours

Chromatogram



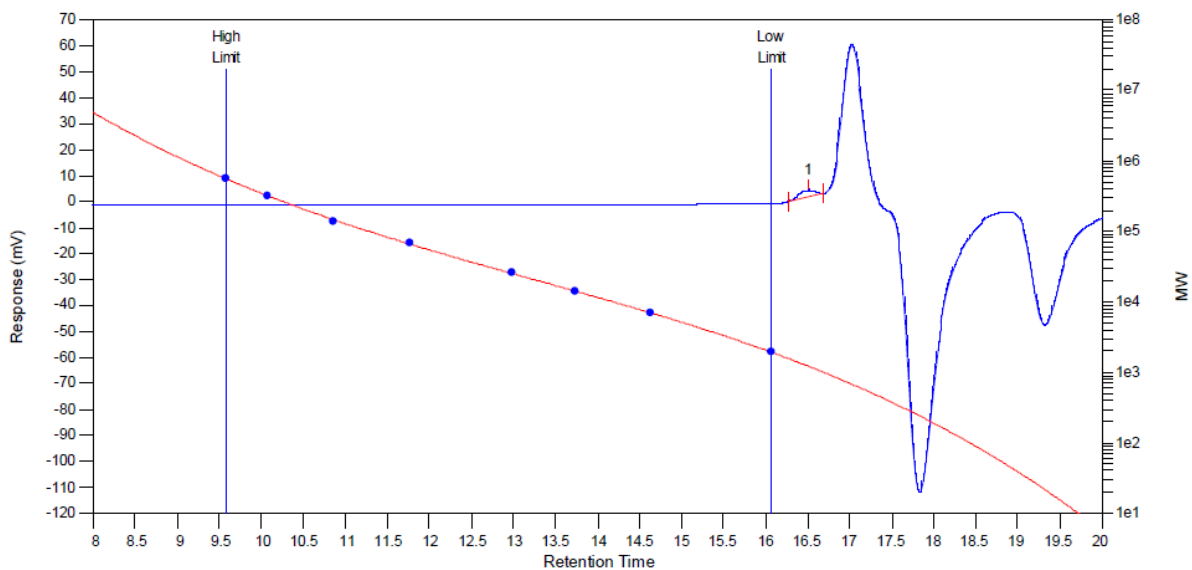
Distribution Plots



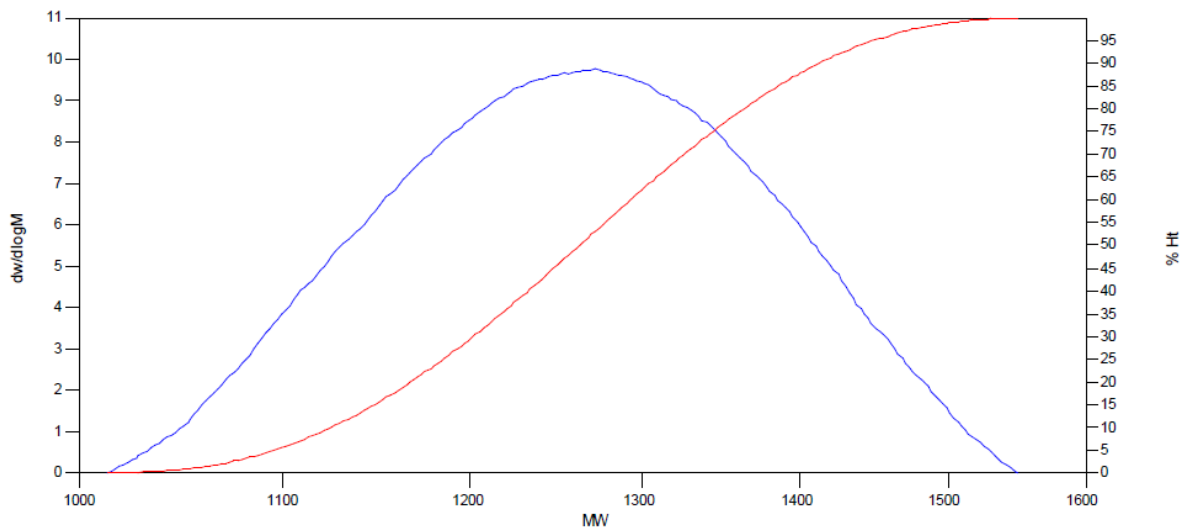
Peak No	Mp	Mn	Mw	Mz	Mz+1	Mv	PD
1	1175	1173	1185	1197	1208	1183	1.01023

Lipase 96 hours

Chromatogram



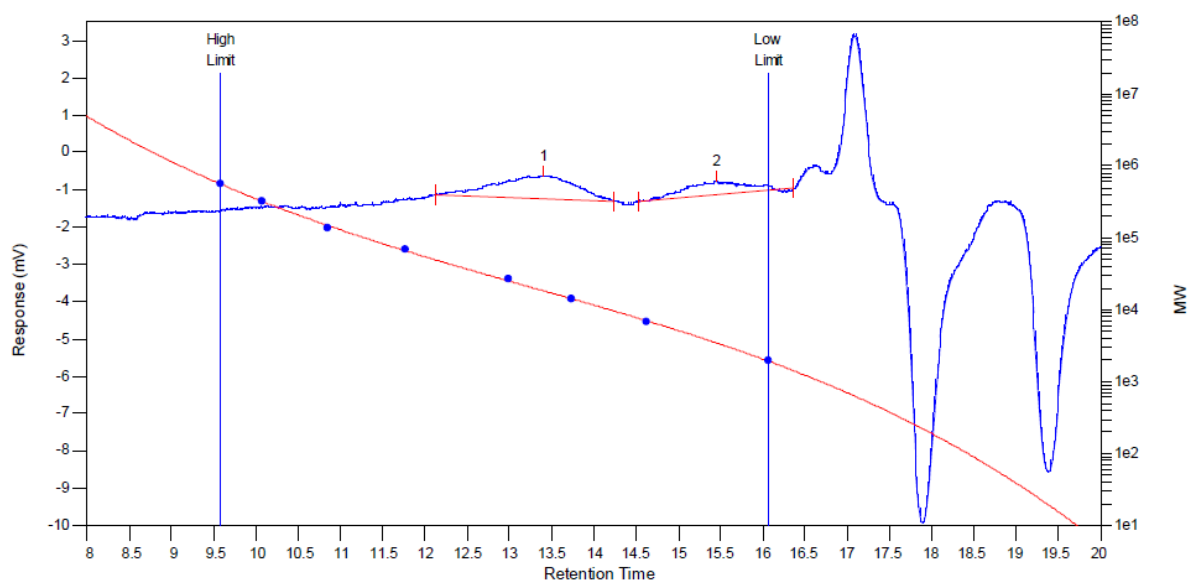
Distribution Plots



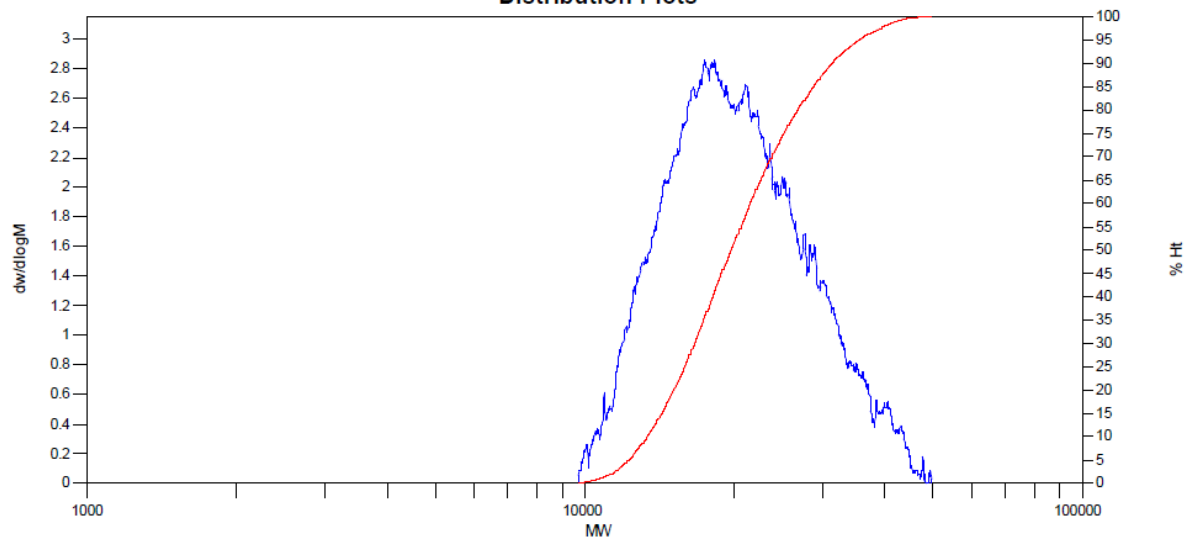
Peak No	Mp	Mn	Mw	Mz	Mz+1	Mv	PD
1	1272	1257	1266	1275	1284	1265	1.00716

Elastase 24 hours

Chromatogram



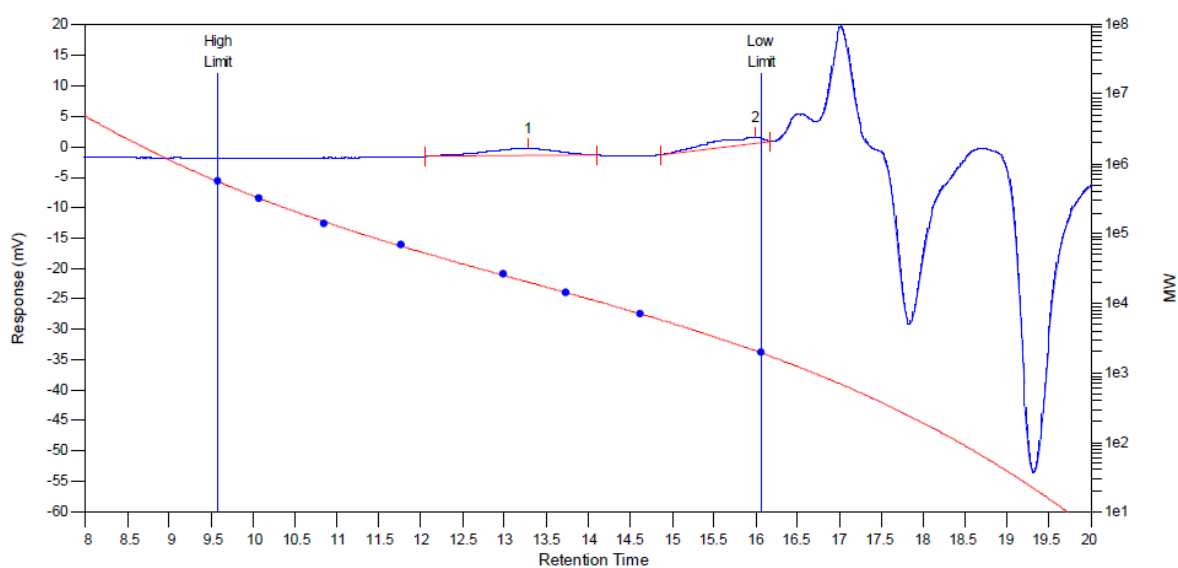
Distribution Plots



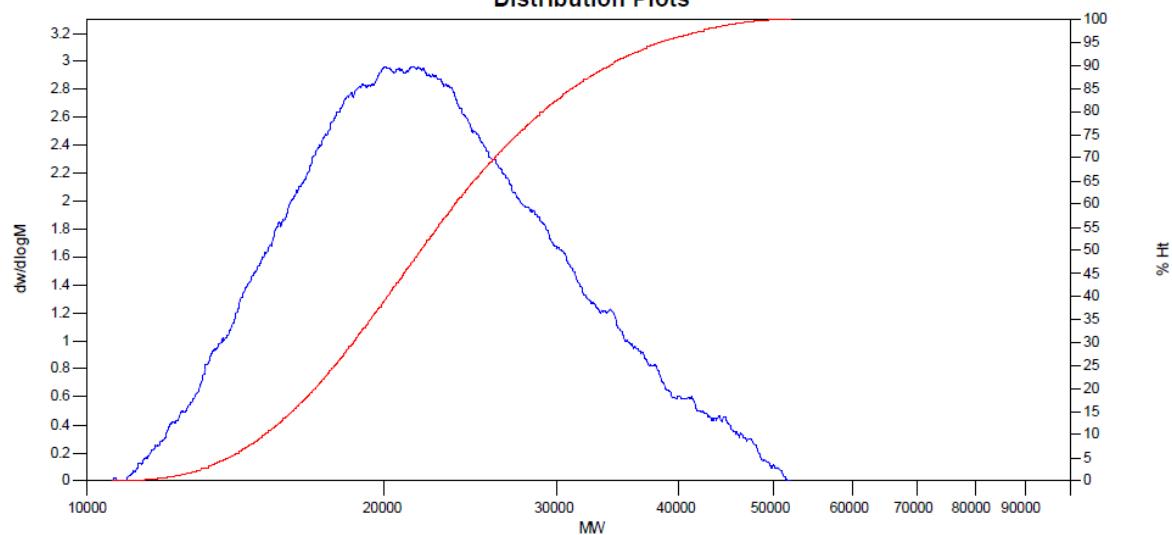
Peak No	Mp	Mn	Mw	Mz	Mz+1	Mv	PD
1	17433	19143	21196	23592	26209	20862	1.10725
2	3455	3438	3774	4114	4439	3724	1.09773

Elastase 48 hours

Chromatogram



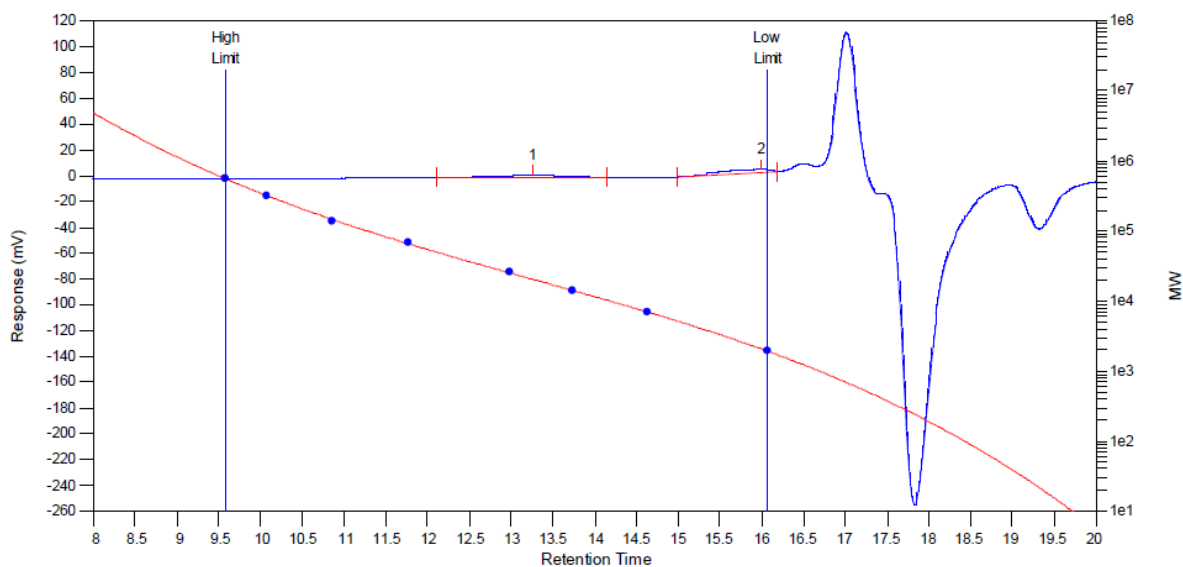
Distribution Plots



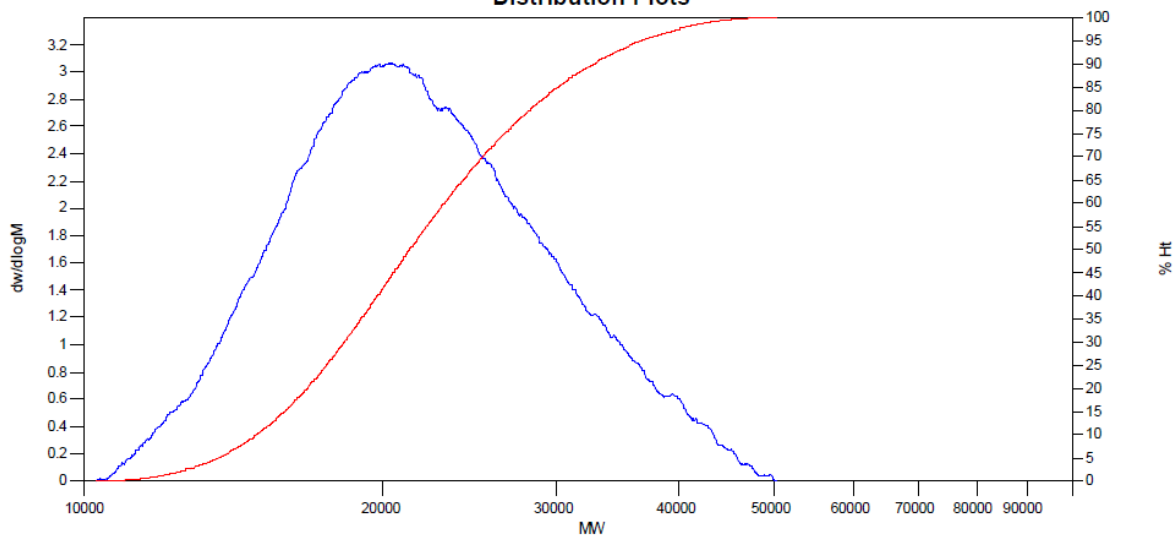
Peak No	Mp	Mn	Mw	Mz	Mz+1	Mv	PD
1	20104	21305	23330	25677	28253	23002	1.09505
2	2901	2905	3115	3337	3559	3083	1.07229

Elastase 96 hours

Chromatogram



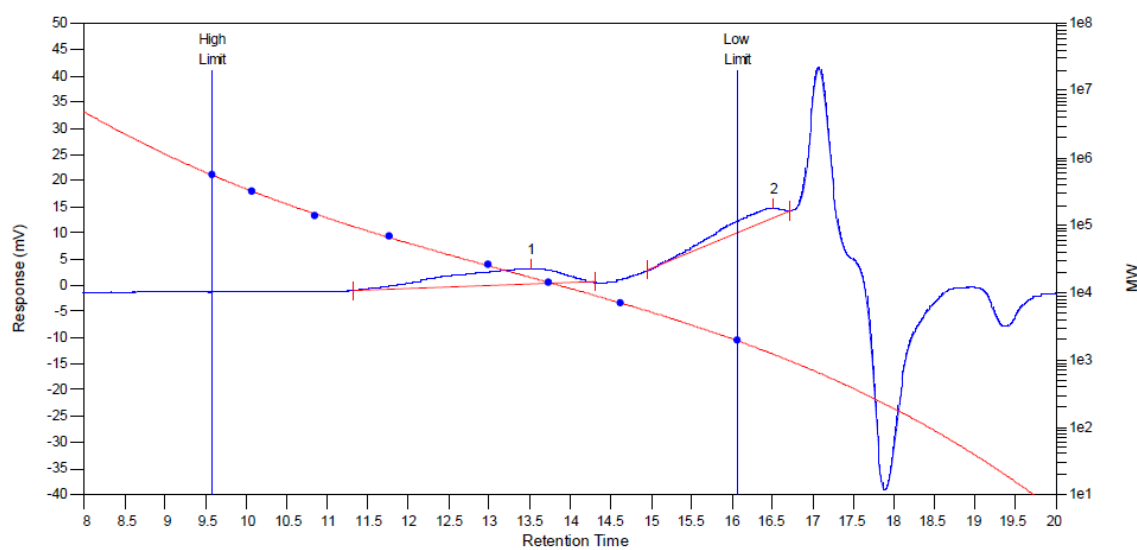
Distribution Plots



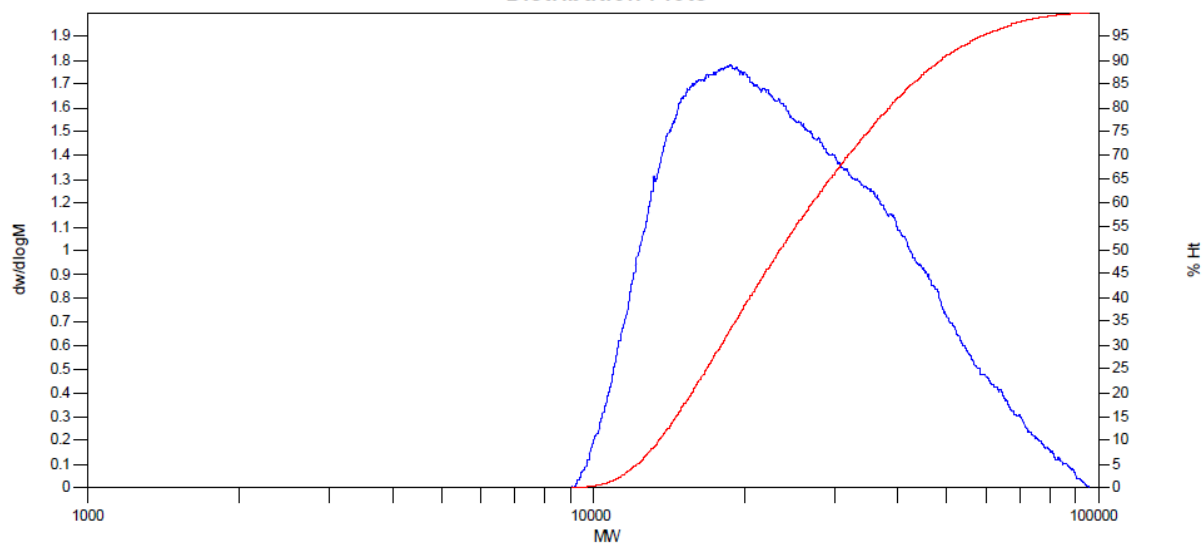
Peak No	Mp	Mn	Mw	Mz	Mz+1	Mv	PD
1	20491	20836	22715	24847	27147	22414	1.09018
2	2101	2678	2830	2993	3159	2806	1.05676

Esterase 24 hours

Chromatogram



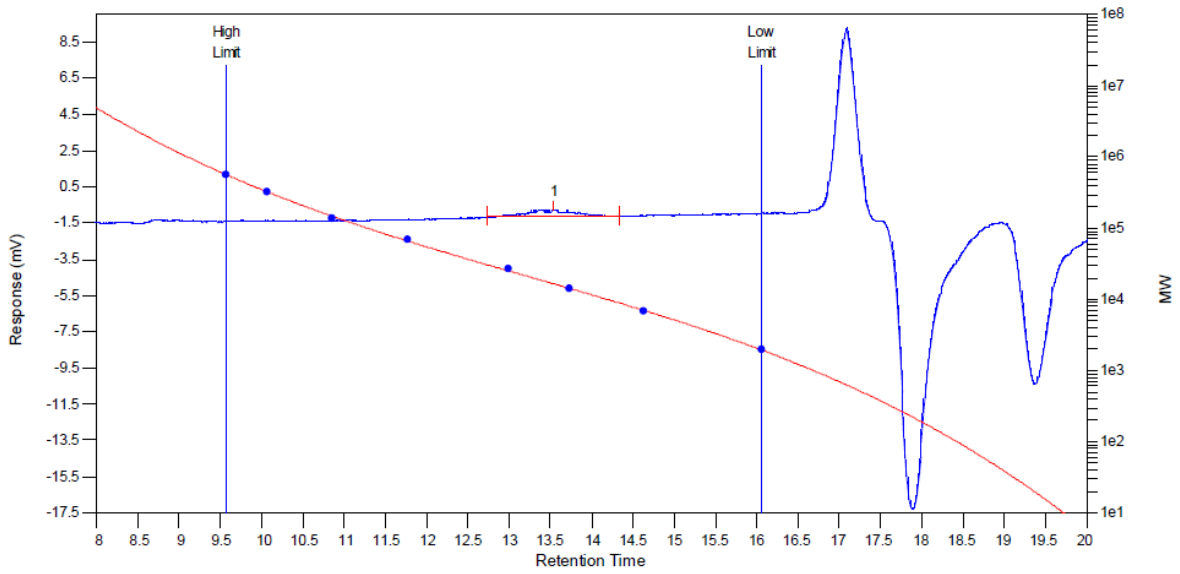
Distribution Plots



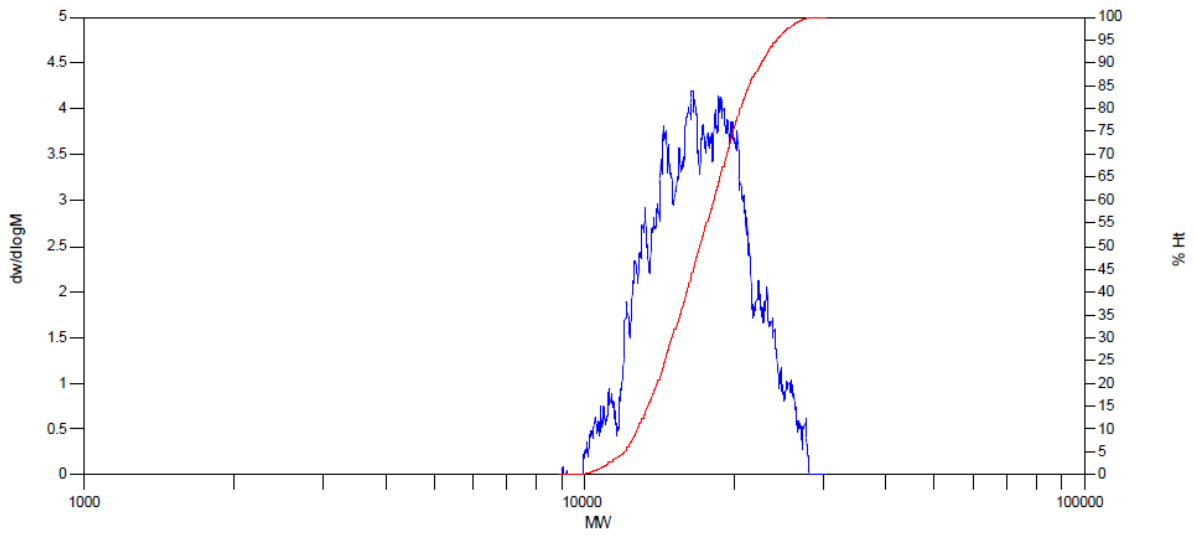
Peak No	Mp	Mn	Mw	Mz	Mz+1	Mv	PD
1	18722	21963	27505	35091	43713	26519	1.25233
2	1880	1860	2103	2390	2702	2063	1.13065

Esterase 72 hours

Chromatogram



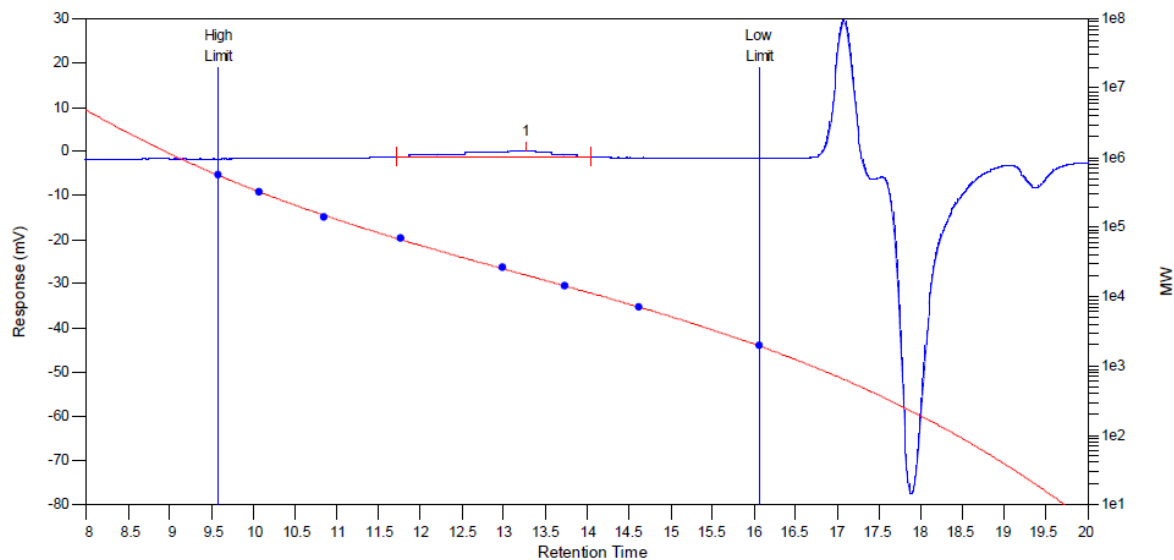
Distribution Plots



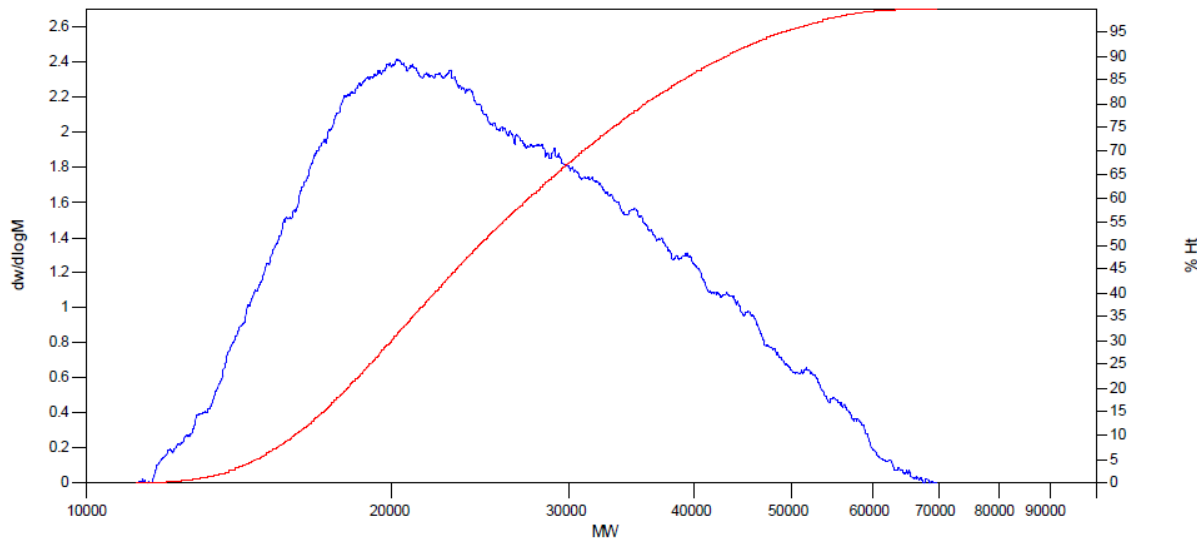
Peak No	Mp	Mn	Mw	Mz	Mz+1	Mv	PD
1	16440	16610	17384	18176	18968	17266	1.0466

Esterase 96 hours

Chromatogram



Distribution Plots



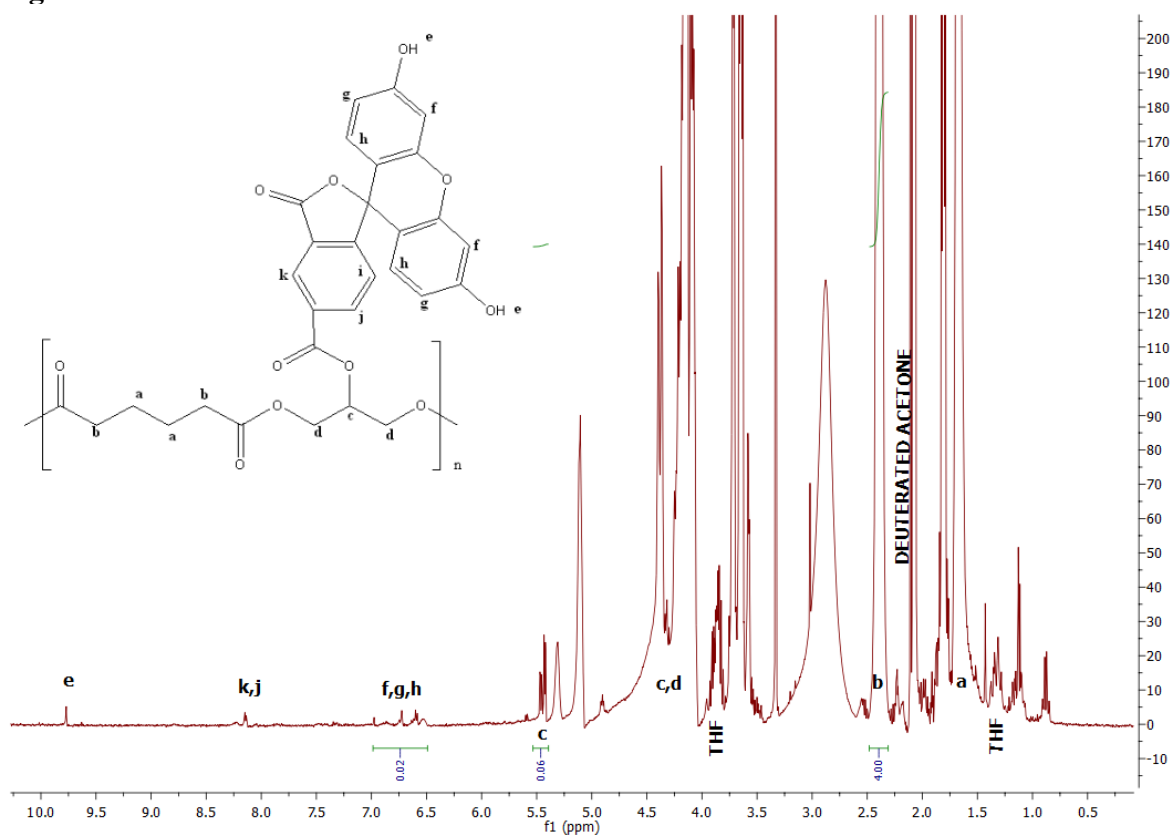
Peak No	Mp	Mn	Mw	Mz	Mz+1	Mv	PD
1	20284	23725	27066	31107	35471	26509	1.14082

References

- [1] Sigma-Aldrich, Elastase (EC 3.4.21.36) continuous spectrophotometric rate assay, (n.d.). <http://www.sigmaaldrich.com/technical-documents/protocols/biology/enzymatic-assay-of-elastase.html> (accessed March 7, 2017).
- [2] Sigma-Aldrich, Enzymatic Assay of Esterase, (n.d.). <http://www.sigmaaldrich.com/technical-documents/protocols/biology/enzymatic-assay-of-esterase.html> (accessed March 7, 2017).
- [3] T.J. Jacks, H.W. Kircher, Fluorometric Assay for the Hydrolytic Activity of Lipase Using Fatty Acyl Esters of 4-Methylumbelliferone, *Anal. Biochem.* 21 (1967) 279–285. doi:10.1016/0003-2697(67)90190-X.
- [4] W. Andlauer, P. Prunier, D. Prim, Fluorometric Method to Assess Lipase Inhibition Activity, *Chim. Int. J. Chem.* 63 (2009) 695–697. doi:10.2533/chimia.2009.695.
- [5] R.N. Roy, Fluorimetric Assay of the Activity of Extracellular Lipases of *Pseudomonas fluorescens* and *Serratia marcescens*, *J. Appl. Bacteriol.* 49 (1980) 265–271. doi:10.1111/j.1365-2672.1980.tb05124.x.
- [6] Sigma-Aldrich, Procedure for Enzymatic Assay of Trypsin (EC 3.4.21.4), (n.d.). <http://www.sigmaaldrich.com/technical-documents/protocols/biology/enzymatic-assay-of-trypsin.html> (accessed March 7, 2017).

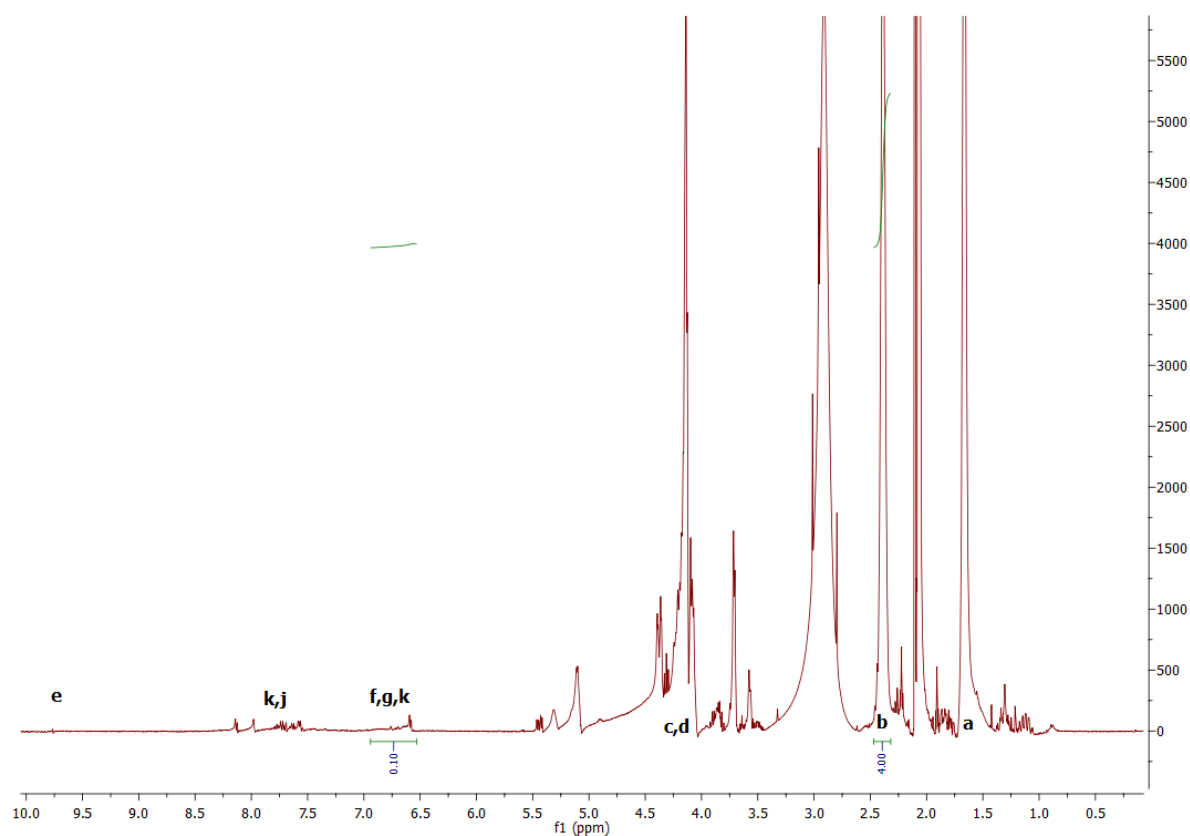
2892
2893
2894 **Figures for Supplementary Information – Appendices A & B**
2895
2896
2897

2898
2899 **Figure A.1**



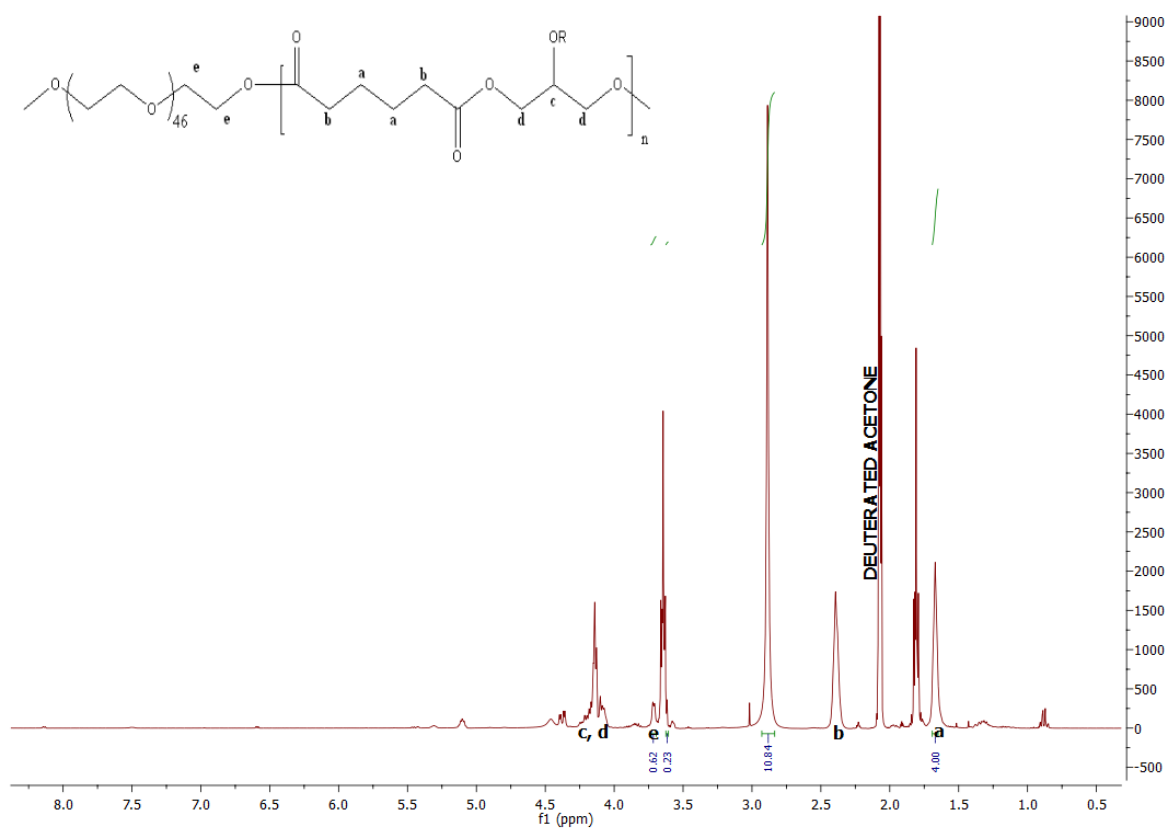
2922
2923
2924
2925 *Fig A.1: NMR Spectrum of PGA-Carboxyfluorescein at Low Substitution.* The peaks relating
2926 to carboxyfluorescein can be seen on the left-hand side of the spectrum whereas those from
2927 PGA are on the right-hand side. The integrals of the peaks labelled 'b', from the PGA, and 'f,
2928 g, h', from the carboxyfluorescein were used to calculate the substitution ratio.
2929
2930
2931
2932
2933
2934
2935
2936
2937
2938
2939
2940
2941
2942
2943
2944
2945
2946
2947
2948
2949
2950

2951
2952
2953 **Figure A.2**
2954
2955



2980 *Fig. A.2: NMR Spectrum of PGA-CF5.* As with PGA-CF [Fig A.1] the integrals of the peaks
2981 labelled 'f, g, h' (carboxyfluorescein) were used to calculate the amount of
2982 carboxyfluorescein, relative to peak b (PGA). The substitution was estimated to be 1.7%.
2983
2984
2985
2986
2987
2988
2989
2990
2991
2992
2993
2994
2995
2996
2997
2998
2999
3000
3001
3002
3003
3004
3005
3006
3007
3008
3009

3010
3011
3012 **Figure A.3**
3013
3014



3039 *Fig. A.3: NMR Spectrum of PGA-PEG.* The peak labelled ‘e’ represents the protons of PEG
3040 adjacent to the ester bond, and was consequently used to confirm the successful coupling and
3041 to predict the substitution ratio.
3042

Figure B.1

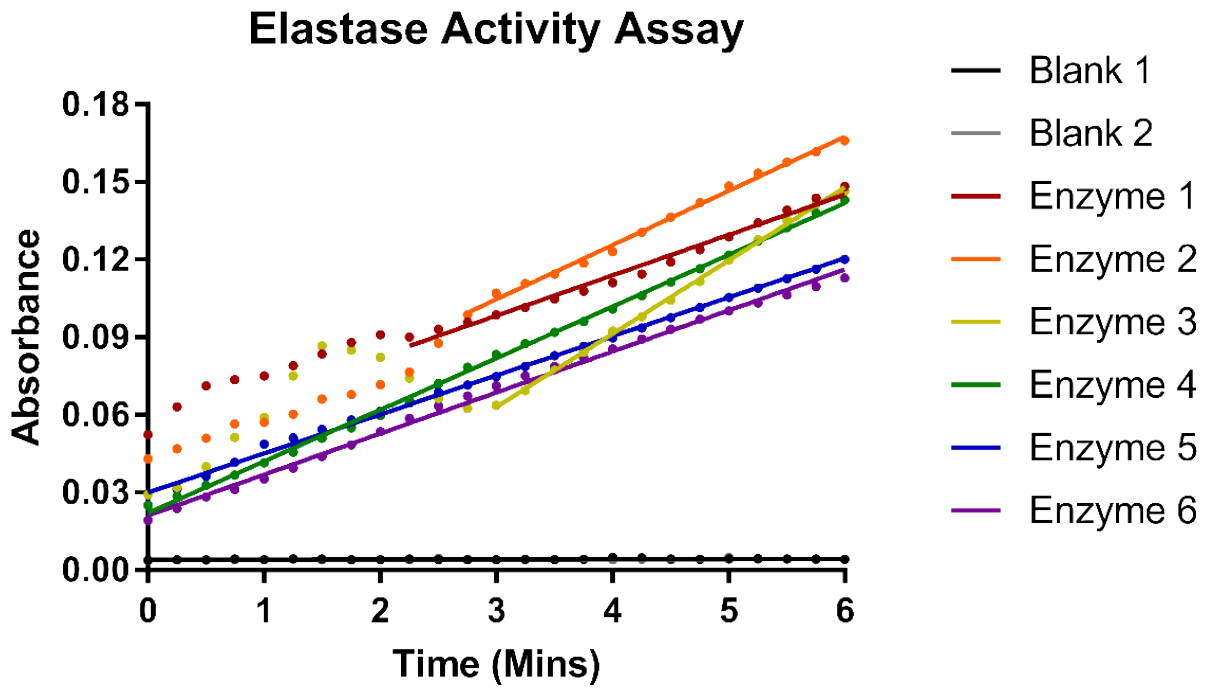


Fig. B.1: Elastase Activity Assay. The change in absorbance at 410 nm is plotted against the time in minutes. Although measurements were taken throughout the 6 minutes only the linear portions are shown here, as recommended in the method. The line of best fit was used to calculate the change in absorbance, and consequently the activity, for each sample. These lines all had a R^2 value >0.985 .

Figure B.2

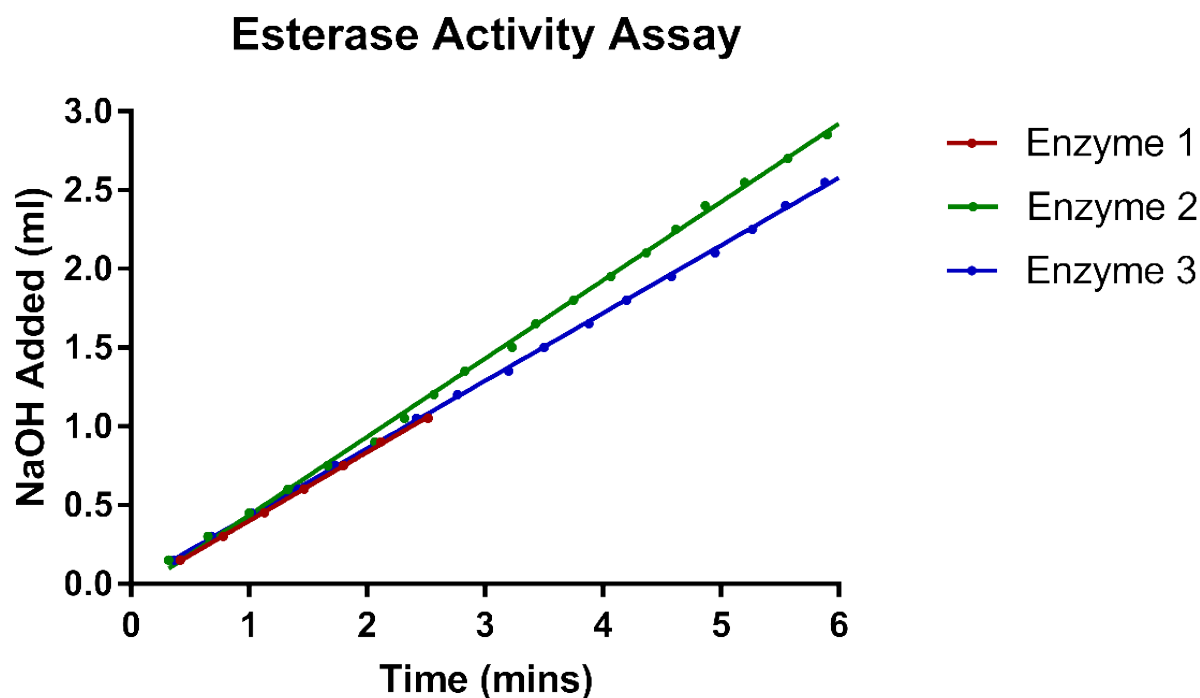


Fig. B.2: Esterase Activity Assay. This graph charts the additions of NaOH made and the time points at which this occurred. As with the elastase activity assay, only the linear portions are shown here to aid clarity. The lines of best fit all had R^2 values >0.99 . The blank is not shown as the pH did not return to 8.0 for the duration of the assay. The gradient of the line was taken as the rate of change and then corrected for the blank; this figure was used to calculate the activity.

Figure B.3

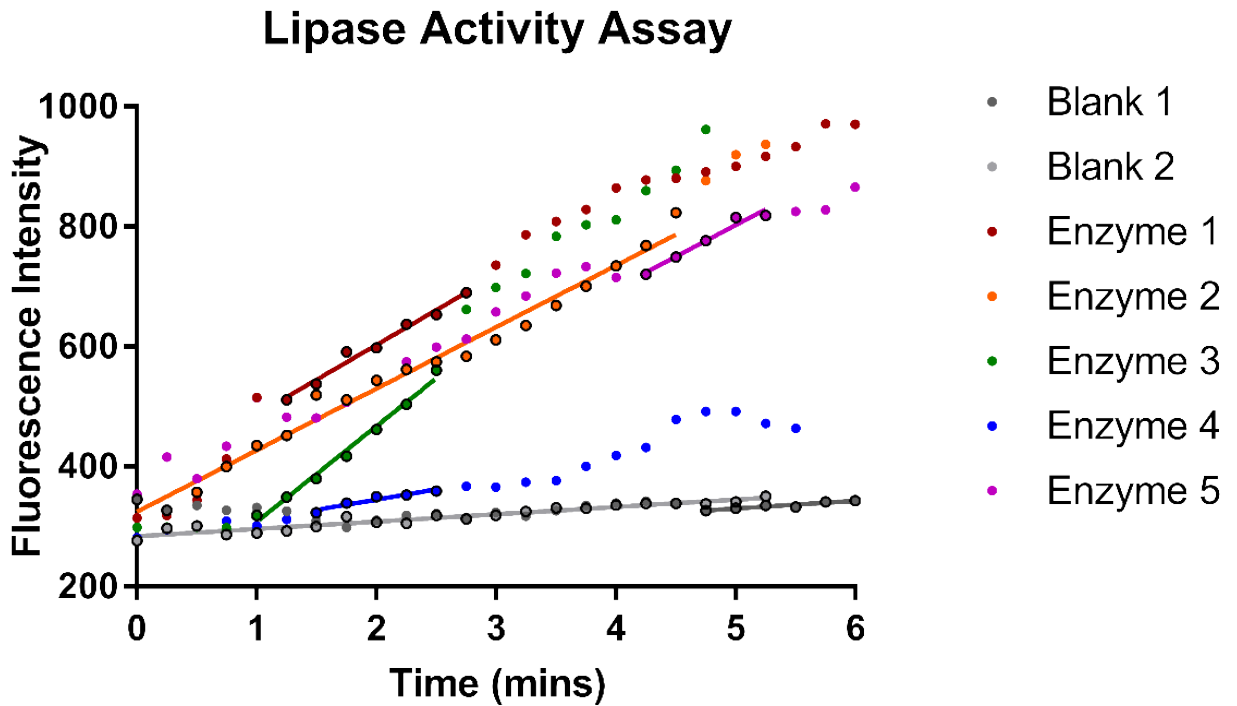


Fig. B.3: Lipase Activity Assay. In this graph the linear portions are highlighted by black borders around the markers; these points were used to calculate the lines of best fit. At least five linear points were used for each sample. Whilst there is quite a difference in the intensities measured this was mainly a result of the time taken to begin the assay; the gradients of the lines for the enzyme samples are relatively similar.

Figure B.4

4-Methylumbelliferone Calibration

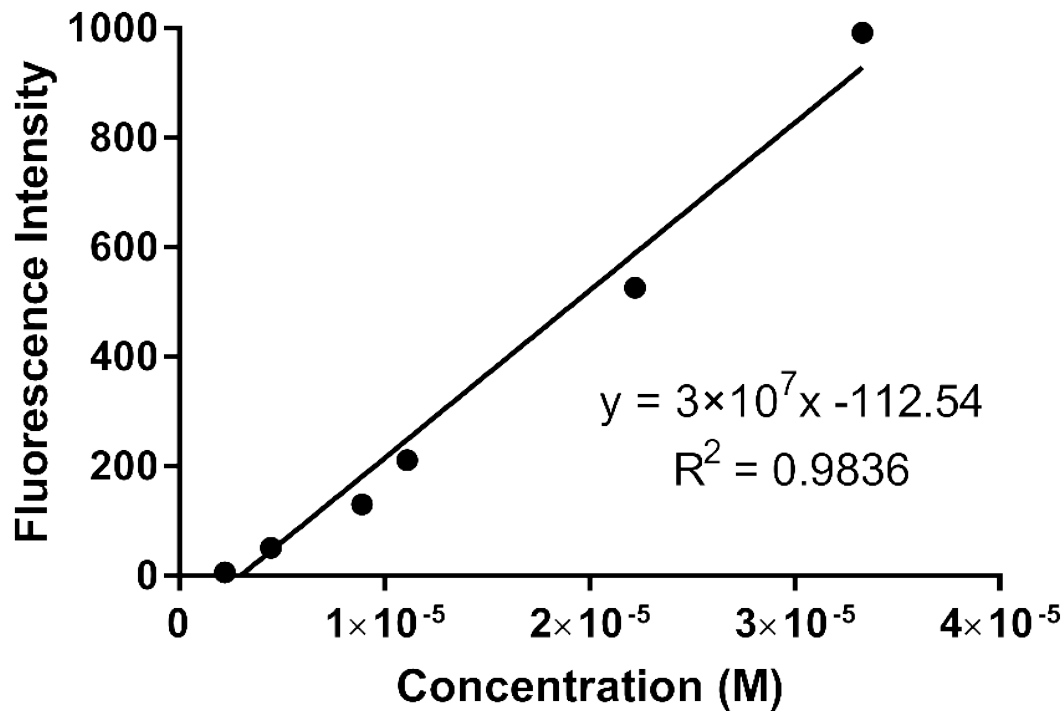


Fig. B.4: Calibration of 4-Methyl Umbelliferone Fluorescence. The graph shows the calibration curve obtained for the fluorescence of 4-MU. The samples tested cover the full range of detectable intensities and a good R^2 value was obtained. Three readings were taken for each concentration; mean values are displayed on this graph. The equation of the line is displayed on the graph.

Figure B.5

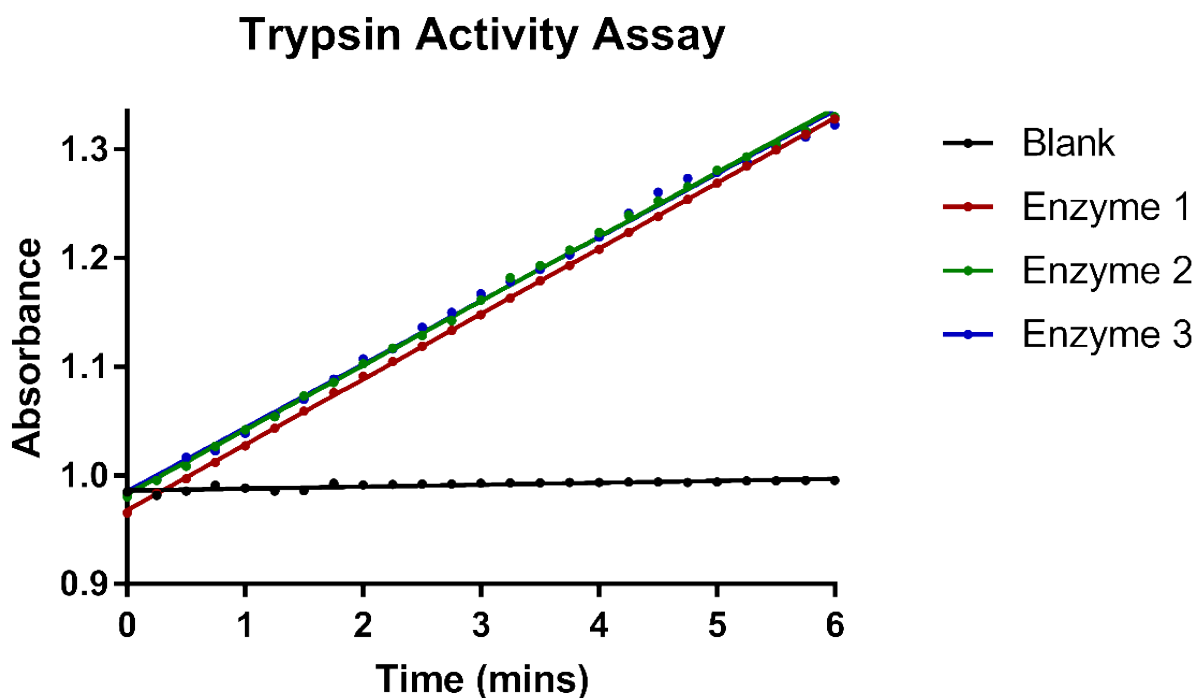


Fig. B.5: Trypsin Activity Assay. The absorbance at 253 nm is plotted against the time in minutes. As with the previous figures, only the linear portion is shown here. The absorbance values for the enzyme samples quickly exceeded 1, however, as the trend showed good linearity and all the lines of best fit had R^2 values >0.99 it was decided it would not be necessary to repeat the measurements.